Original Article

MOLECULAR METABOLISM

Hypophagia induced by salmon calcitonin, but not by amylin, is partially driven by malaise and is mediated by CGRP neurons

Lavinia Boccia [1], Tito Borner [2,3], Misgana Y. Ghidewon [4], Patricia Kulka [1], Chiara Piffaretti [1], Sarah A. Doebley [2], Bart C. De Jonghe [2,3], Harvey J. Grill [4], Thomas A. Lutz [1,5], Christelle Le Foll [1,*,5]

ABSTRACT

Objective: The behavioral mechanisms and the neuronal pathways mediated by amylin and its long-acting analog sCT (salmon calcitonin) are not fully understood and it is unclear to what extent sCT and amylin engage overlapping or distinct neuronal subpopulations to reduce food intake. We here hypothesize that amylin and sCT recruit different neuronal population to mediate their anorectic effects.

Methods: Viral approaches were used to inhibit calcitonin gene-related peptide (CGRP) lateral parabrachial nucleus (LPBN) neurons and assess their role in amylin's and sCT's ability to decrease food intake in mice. In addition, to test the involvement of LPBN CGRP neuropeptidergic signaling in the mediation of amylin and sCT's effects, a LPBN site-specific knockdown was performed in rats. To deeper investigate whether the greater anorectic effect of sCT compared to amylin is due do the recruitment of additional neuronal pathways related to malaise multiple and distinct animal models tested whether amylin and sCT induce conditioned avoidance, nausea, emesis, and conditioned affective taste aversion.

Results: Our results indicate that permanent or transient inhibition of CGRP neurons in LPBN blunts sCT-, but not amylin-induced anorexia and neuronal activation. Importantly, sCT but not amylin induces behaviors indicative of malaise including conditioned affective aversion, nausea, emesis, and conditioned avoidance; the latter mediated by $CGRP^{LPBN}$ neurons.

Conclusions: Together, the present study highlights that although amylin and sCT comparably decrease food intake, sCT is distinctive from amylin in the activation of anorectic neuronal pathways associated with malaise.

Keywords Calcitonin gene-related peptides neurons; Hindbrain; Lateral parabrachial nucleus; Aversion; Emesis; *Suncus murinus*

1. INTRODUCTION

Amylin is a 37-amino-acid peptide, produced by pancreatic β-cells and co-secreted with insulin in response to meal ingestion [1]. Amylin's main function is to reduce eating by promoting satiation (i.e., the processes that terminate an ongoing meal) via direct central action [1,2]. The amylin receptor (AMY) is composed of the calcitonin receptor (CTR) [1] which heterodimerizes with one of the three receptor activity-modifying proteins (RAMP1, 2, and 3) [3,4]. These receptor components can be found in brain nuclei involved in the control of feeding and metabolism including the area postrema (AP) [5], the nucleus of the solitary tract (NTS), and the arcuate nucleus of the hypothalamus (ARC) [6]. Amylin's satiation effect is primarily mediated by the activation of neurons in the AP which then signal to downstream nuclei, such as the lateral parabrachial nucleus (LPBN) [1,7,8,9,10] and central nucleus of the amygdala (CeA) [11,12].

Salmon calcitonin (sCT) is a 32-amino-acid peptide structurally similar to amylin [1,13]. sCT displays higher retention at the AMY receptor compared to amylin, which is considered the reason for its longer and more potent hypophagic effect [1,12,14,15,16,17]. It remains to be elucidated whether other neurological and behavioral processes, in addition to enhanced satiation, contribute to differential effects of amylin and sCT.

The LPBN receives a variety of visceral signals from the caudal hindbrain and also communicates with forebrain areas, including the CeA [12,18,19]. Ablation of the LPBN reduces the anorectic effect of amylin and its ability to activate CeA neurons [7]. The LPBN comprises a heterogeneous neuronal population [20] including a sub-population of neurons expressing calcitonin gene-related peptide (CGRP) which play an important role in food intake control. Optogenetic or chemogenetic activation of $CGRP^{LPBN}$ neurons results in meal termination, and conversely, their inactivation increases meal size and meal duration [21]. Inhibition of $CGRP^{LPBN}$ neurons also abolishes the effects of meal-related satiation peptides, like cholecystokinin (CCK), glucagon-like peptide-1 (GLP-1) analog Exendin-4 (Ex4), and leptin [21]. Importantly, previous studies also showed amylin-induced Fos

[1]Institute of Veterinary Physiology, Vetsuisse Faculty, University of Zurich (UZH), 8057, Zurich, Switzerland [2]Department of Biobehavioral Health Sciences, University of Pennsylvania, School of Nursing, Philadelphia, PA 19104, United States [3]Department of Psychiatry, University of Pennsylvania, Perelman School of Medicine, Philadelphia, PA 19104, United States [4]Institute of Diabetes, Obesity and Metabolism and School of Arts and Sciences, University of Pennsylvania, Philadelphia, PA 19104, United States

[5] These last authors share equal contribution.

*Corresponding author. Institute of Veterinary Physiology, University of Zurich Winterthurerstrasse 260 8057, Zurich, Switzerland. E-mail: christelle.lefoll@uzh.ch (C. Le Foll).

Received December 8, 2021 • Revision received January 7, 2022 • Accepted January 19, 2022 • Available online 25 January 2022

https://doi.org/10.1016/j.molmet.2022.101444

expression in those neurons [9,22], but the functional role of $CGRP^{LPBN}$ neurons in the mediation of amylin's and sCT's anorexia has not yet been investigated. CGRP neurons are not just involved in modulating physiological satiation, but they relay a variety of signals (food poisoning, pain, foot shock, itch, etc.) and taste memories [23]. Activation of CGRP neurons is sufficient to condition a taste avoidance while silencing them reduces the avoidance conditioned by the toxin lithium chloride (LiCl) [24]. Interestingly, it remains to be evaluated whether the feeding suppression by amylin and/or sCT involves the induction of visceral malaise across multiple doses and species, as is the case for other anti-obesity medications, such as GLP-1R agonists [25,26]. We hypothesize that sCT, not amylin, activates $CGRP^{LPBN}$ neurons activation which contributes to anorexia partially via the induction of malaise.

Interestingly, CGRP seems to play a role in energy homeostasis [27,28,29]. CGRP protein knockout mice were protected from obesity and displayed improved glucose control and insulin sensitivity [27,28,29]. Nevertheless, it is unclear whether CGRP as a neuropeptide also plays a role in mediating amylin's and sCT's anorectic effect and whether it contributes to the neuronal activation of LPBN downstream sites. It is important to know that $CGRP^{LPBN}$ neurons in addition to the release of CGRP, also release different neurotransmitters and neuropeptides, such as tachykinins and glutamate [23].

Here, we used viral approaches to inhibit $CGRP^{LPBN}$ neurons and assessed their role in amylin's and sCT's ability to decrease food intake in mice. In addition, to test the involvement of LPBN CGRP neuropeptidergic signaling in the mediation of amylin's and sCT's effects, an LPBN site-specific knockdown was performed in rats. Notably, to more thoroughly investigate whether the greater anorectic effect of sCT compared to amylin is due to the recruitment of additional neuronal pathways related to malaise, we tested in multiple, distinct models whether amylin and sCT induce conditioned avoidance, nausea, emesis, and conditioned affective taste aversion.

2. METHODS

2.1. Experimental models and subject details

All procedures were approved by the Veterinary Office of the Canton of Zurich and the Institutional Care and Use Committee of the University of Pennsylvania.

2.1.1. Mice

Male and female heterozygous Calca Cre/+ mice ($Calca^{tm1.1(cre/EGFP)Rpa}$ MGI:5559692), were generated as explained by Carter et al. [22] and backcrossed onto a C57Bl/6 background. Mice were 12–16 weeks old at the start of the experimental procedures. Calca-cre mice were genotyped using a standard protocol and primers are indicated in the star method table.

For all studies, mice were processed in the order of their toe clip number, which was randomly assigned at the time of sampling for genotyping. Prior to stereotaxic surgery, mice were group-housed and maintained with a standard chow diet (Kliba 3430) and water available ad libitum with a 12-h light–dark cycle at 22 °C (lights off at 11:00). Mice were randomly assigned to either the experimental or control group within each litter.

2.1.2. Rats

Male Sprague–Dawley rats weighing between 250 and 275 g at the time of the arrival were used (Janvier Elevage, Le Genest-Saint-Isle, France). Rats were acclimated for one week before the experiment/surgery and maintained on standard rodent chow ad libitum. Two cohorts of rats were used. The first cohort of rats was maintained on a standard chow diet ad libitum, except for the periods of food deprivation described below (n = 32, n = 16/group). The second cohort of rats was kept under a 45% high-fat diet (EF D12451, SSNIFF diet, Germany) for 8 weeks, before starting the trials (n = 32, n = 16/group).

2.1.3. Shrews

Adult male shrews (*Suncus murinus*) weighing ~50–80 g (n = 29 total), were bred and maintained at the University of Pennsylvania; they derive from a Taiwanese strain and initially were supplied by the Chinese University of Hong Kong. Shrews were singly housed in plastic cages (37.3 × 23.4 × 14 cm, Innovive) under a 12-h light/dark cycle in a temperature- and humidity-controlled environment. Shrews were fed ad libitum with a mixture of feline (75%, Laboratory Feline Diet 5003, Lab Diet) and mink food (25%, High-Density Ferret Diet 5LI4, Lab Diet) and had ad libitum access to tap water except where noted. Shrews were habituated to single housing in their home cage and intraperitoneal (i.p.) injections at least 1 wk prior to experimentation.

2.2. Drugs, drug formulation, and route of administration

Amylin (4,030,201, Bachem AG, Bubendorf, Switzerland) and sCT (4,033,011, Bachem AG) were reconstituted with sterile 0.9% saline, the injected volume was 1 mL/kg in rats and 10 mL/kg in mice and shrews. All animals were naïve to any experimental drug and test prior to the beginning of the experiment. The animals were habituated to i.p. injections by injecting saline for 3–5 days before testing. Feeding trials were performed at dark onset in a randomized, crossover manner so that each animal was examined under all treatment conditions with at least 3 (rodents) and 7 (shrews) days of recovery between trials.

In experiments 1 and 2, upon 12-h fasting in the light phase, animals received injections of either saline, amylin (50 or 500 μg/kg), or sCT (5 μg/kg [rats] 10 μg/kg [mice] i.p.) just before dark onset. Specifically, the dose of sCT was chosen based on our prior work that showed that 5 μg/kg in rats and 10 μg/kg in mice is sufficient in mice to induce anorexia at 1, 2, 4, and 24-h [9,30]. In experiment 1 (temporary inhibition of $CGRP^{LPBN}$ neurons) the animals were pretreated with vehicle or CNO (1 mg/kg i.p.) 15 min prior to the peptide injection for the baseline measurement and before the treatments. Each animal always received the same pre-treatment. In experiments 4 and 5, after 2 h of fasting, animals received either saline, amylin (500 μg/kg), or sCT (5 μg/kg) i.p.

2.3. Food intake monitoring

Animals (mice in an experiment related to Figure 1 and rats in an experiment related to Figure 2) were housed in BioDAQ cages (Research Diet, NJ, USA). After the treatment administration, food was returned, and meal patterns were recorded automatically in BioDAQ cages for 24 h. In experiment 4, food intake was manually measured at 1, 4, and 24 h.

2.4. Brain processing

After a 12-h fast in the light phase, animals were injected at dark onset with the treatments (specific details for each experiment are described below). Ninety min later animals were deeply anesthetized (Pentobarbital 100 mg/kg, i.p) and transcardially perfused with cold 0.1 M of phosphate buffer (PB) for 1.5 min followed by 4% of paraformaldehyde (PFA) in PB for 2.5 min. Brains were removed and postfixed overnight in 4% of PFA and cryoprotected in 20% of sucrose-PB for 24 h. Brains were frozen on dry ice and stored at −80 °C until sectioning. Brain sections were cut on a cryostat (CM3050S, Leica Biosystems, Germany), mounted on Superfrost Plus slides (Thermo Fisher Scientific,

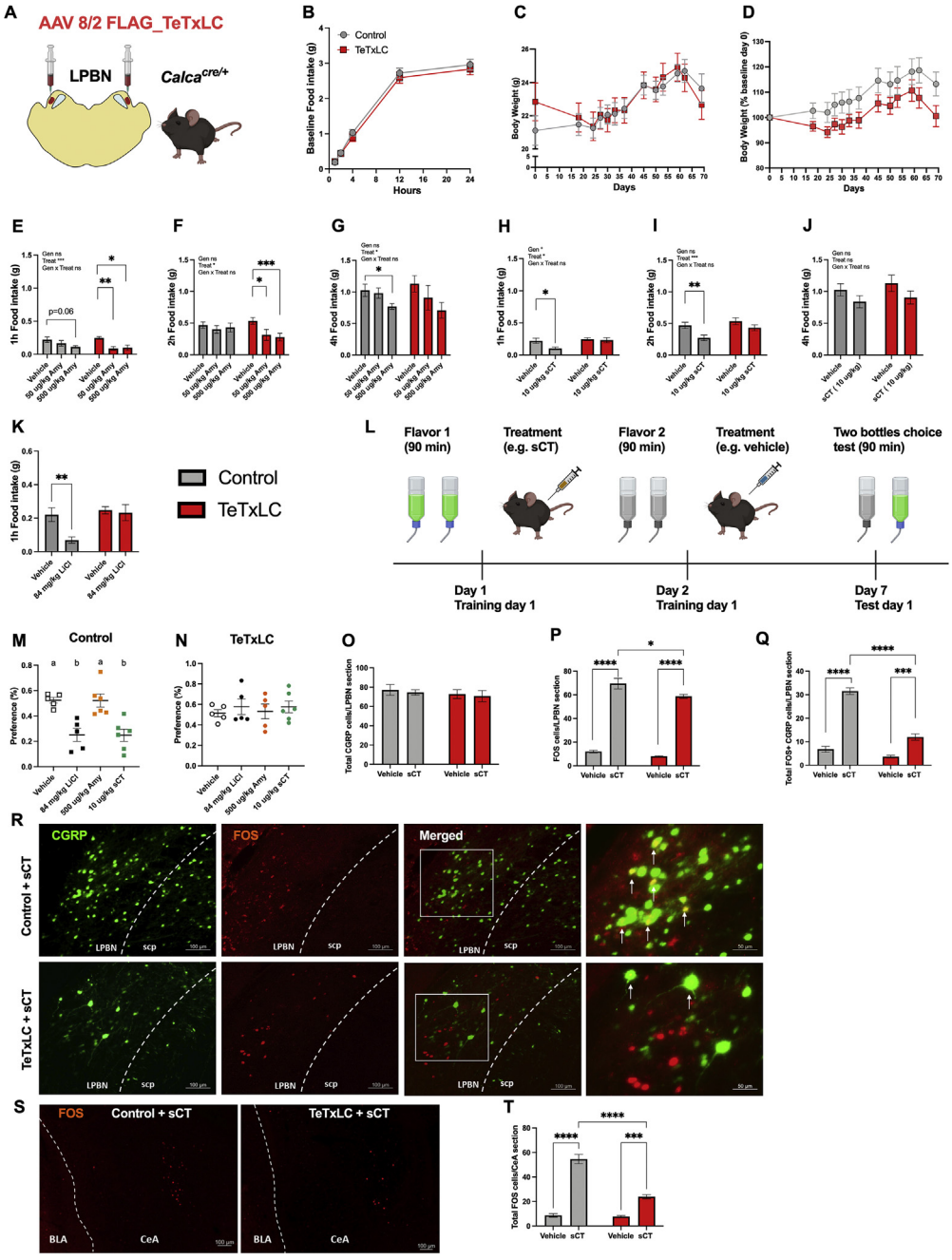

Figure 1: Silencing CGRP^{LPBN} neurons reduced sCT anorectic effect, conditioned avoidance and neuronal activation in LPBN and CeA. (A) Schematic representation of AAV tetanus toxin virus injected in the LPBN of Calca-cre transgenic mice to specifically silence CGRP^{LPBN} neurons. (B) Cumulative baseline 24-hour food intake determined in BioDaq cages. (C) Body weight from Day 0 (surgery Day) until day 69 (sacrifice Day). (D) Body weight expressed as percent of day 0 during the experiment. (E–G) Cumulative food intake in 12-hour fasted control or TeTxLC (n = 11/group) mice after acute injection of vehicle (0.9% NaCl) or amylin (50 μg/kg and 500 μg/kg; i.p.) at 1 h (E), 2 h (F) and 4 h (G). (H–J) Cumulative food intake in 12-hour fasted control or TeTxLC (n = 11/group) mice after acute injection of vehicle or sCT (10 μg/kg) at 1 h (H), 2 h (I) and 4 h (J). (K) Effect of LiCl (84 mg/kg; i.p.) on 1-hour cumulative food intake in 12-hour fasted control or TeTxLC (n = 11/group) mice. (L) Schematic representation of the two bottles choice test paradigm: in the training days, the mice learned to associate a novel taste (e.g., cherry) with the treatment (e.g., sCT) and another novel taste (e.g. grape) with the vehicle. On the test day the animal freely chooses between the taste associated with vehicle or the one associated with the treatment. (M) Condition avoidance in control mice after vehicle (0.9% NaCl, n = 5), LiCl (84 mg/kg; i.p, n = 5), amylin (500 μg/kg; i.p, n = 6) or sCT (10 μg/kg; i.p, n = 6). (N) Condition avoidance in TeTxLC mice after vehicle (0.9% NaCl, n = 5), LiCl (84 mg/kg; i.p, n = 5), amylin (500 μg/kg; i.p, n = 5) and sCT (10 μg/kg; i.p, n = 6). (O–T) Acute administration of vehicle or sCT (10 μg/kg; i.p) in 12-hour fasted control or TeTxLC mice (n = 11/group). (O) Total number of CGRP-positive cells per LPBN section. (P) Total number of Fos positive cells per LPBN section. (Q) Total Fos + CGRP cells per LPBN section. (R) Representative immunofluorescent images showing CGRP neurons (green), Fos cells (red) and CGRP/Fos positive cells (yellow) in the LPBN. (S) Representative immunofluorescent images showing Fos cells (red) in CeA. (T) Total Fos cells per CeA section (n = 11/group). All data are expressed as mean ± SEM. Data in (A–K), (O–Q) and (T) were analyzed using a two-way ANOVA followed by Sidak's post hoc tests. Data in (M–N) were analyzed using a one-way ANOVA test. *p < 0.05; **p < 0.01; ***p < 0.001; ****p < 0.0001. (M) [a,b] Data points with differing superscripts differ from each other at the p < 0.01 level. See also Figs. S1 and S2.

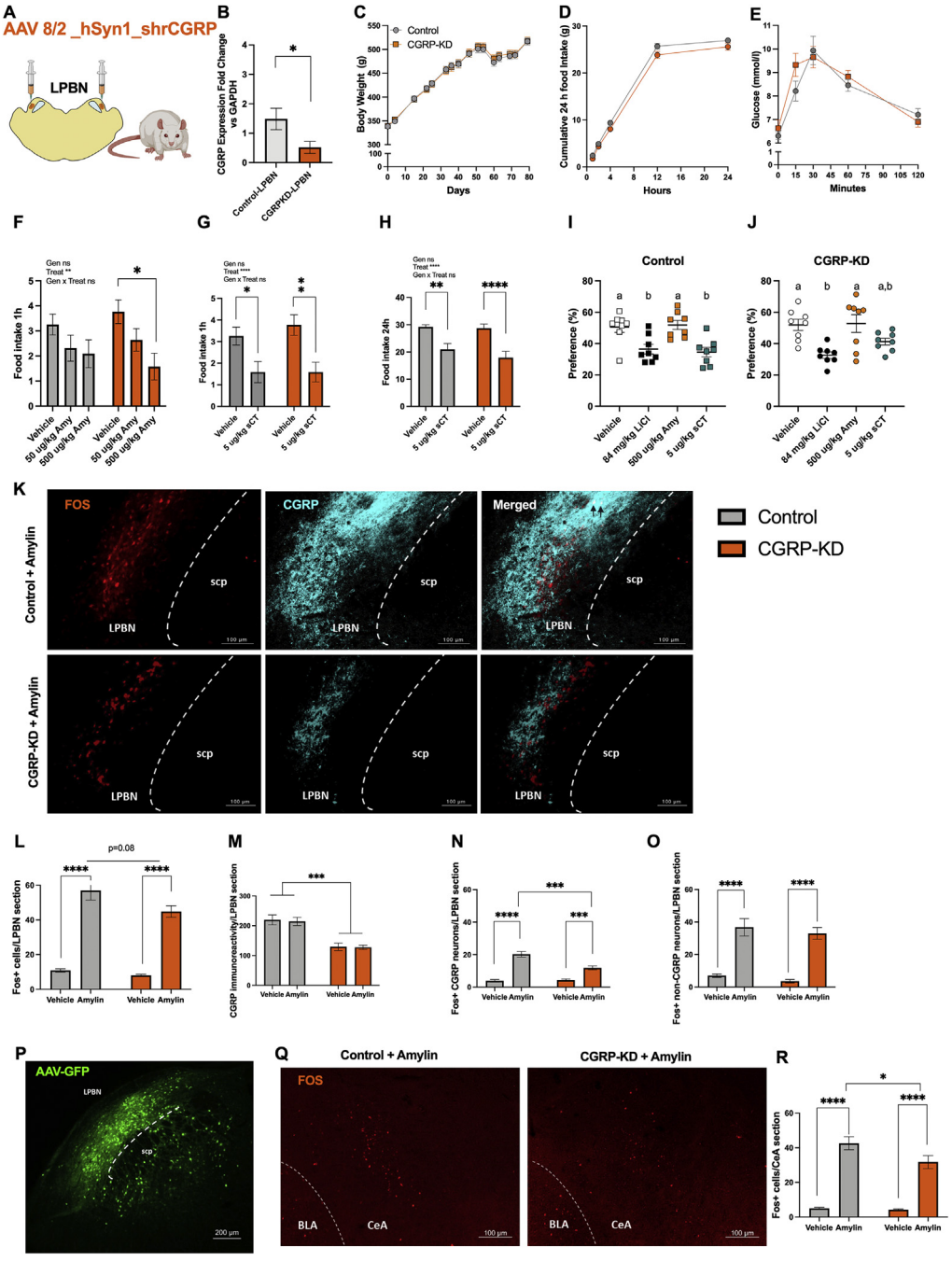

Figure 2: Reduction of CGRP m-RNA level in LPBN neurons did not alter amylin and sCT's effects in lean rats. (A) Schematic representation of AAV short hairpin RNA virus injected in the LPBN of lean rats to specifically knock down CGRP peptide. (B) Expression fold change of CGRP in rats injected with an AAV-GFP control (n = 8) or an AAV-shrRNA-CGRP (n = 9). (C) Body weight in control (n = 16) and CGRP-KD (n = 16) from day 0 (surgery day) until day 79 (sacrifice day), on day 51 the OGTT test was performed and for this reason it is possible to observe a general body weight decrease in the following days, that was then recovered. (D) Cumulative baseline 24-hour food intake determined in BioDaq cages. (E) Plasma glucose concentration over 120 min during an oral glucose tolerance test (2 g/kg). (F) 1 h cumulative food intake in 12-hour fasted control and CGRP KD rats (n = 16/group) after acute injection of vehicle or amylin (50 ug/kg and 500 ug/kg; i.p.). (G–H) Cumulative food intake in 12-hour fasted control and CGRP KD rats (n = 16/group) after acute injection of vehicle or sCT (10 μg/kg; i.p.) at 1 h (G) and 24 h (H). (I) Conditioned avoidance in control rats after LiCl (84 mg/kg; i.p) or sCT (10 μg/kg; i.p). (J) Conditioned avoidance in CGRP KD rats after LiCl (84 mg/kg; i.p) or sCT (10 μg/kg; i.p). (K–R) Acute administration of vehicle or amylin (50 μg/kg; i.p.) in 12-hour fasted control or CGRP-KD rats. (K) Representative immunofluorescent images showing CGRP neurons (cyan), Fos (red) cells and CGRP/Fos positive cells (white) in LPBN. (L) Total Fos cells per LPBN section. (M) CGRP immunoreactivity per LPBN section. (N) Total Fos+/CGRP cells per LPBN section. (O) Total Fos in non-CGRP cells per LPBN section. (P) Example image of AAV-mediated GFP expression (green) in the LPBN. (Q) Representative immunofluorescent images showing Fos cells (red) in the CeA. (R) Total Fos cells per CeA section. All data expressed as mean ± SEM. Data in (B) were analyzed with Student t-test. Data in (C–H), (L–O) and (R) were analyzed using a two-way ANOVA, followed by Sidak's post hoc tests. Data in (I–J) were analyzed using a one-way ANOVA test. *$p < 0.05$; **$p < 0.01$; ***$p < 0.001$; ****$p < 0.0001$. (I–J) ^{a,b} Data points with differing superscripts differ from each other at the $p < 0.05$ (I: veh vs LiCl) or $p < 0.01$ level (I: veh vs sCT, LiCl vs Amy, Amy vs sCT; J: veh vs LiCl, LiCl vs Amy). See also Figs. S3 and S4.

Reinach, Switzerland), and cryoprotected in 50% of PB, 30% of ethylene glycol, 20% of glycerol, and subsequently stored at −20 °C.

2.5. Brain immunohistochemistry

2.5.1. Fos

Blocking of the rodent brain sections was performed with 0.4% triton - 4% normal goat serum (NGS) in PBS for 2 h at room temperature. AP/NTS, LPBN, and CeA sections were incubated at 4 °C for 48 h with rabbit anti-Fos (1:500, 2250, Cell signaling) antibody, and then after rinsing, incubated with goat anti-rabbit Alexa Fluor 488 (1:200,111-545-144, Jackson Immunoresearch) or goat anti-rabbit Alexa Fluor CY3 (1:200, 111-165-144, Jackson Immunoresearch) for 2 h at room temperature. After thorough washing in PBS, the sections were counterstained with DAPI (0.25 μg/mL, 5 min), mounted immediately and coverslipped with Vectashield antifade Mounting Medium (H-1400, Vectorlabs, Burlingame, CA, USA).

2.5.2. Fos/CGRP

Following blocking, LPBN sections were incubated at 4 °C for 48 h with rabbit anti-Fos (1:500, 2250, Cell signaling) and mouse anti-CGRP [31] (1:1000, UCLA/CURE Digestive Research Center, Los Angeles, CA, USA) primary antibodies, and then after rinsing, incubated with goat anti-rabbit Alexa Fluor CY3 and goat anti-mouse 647 (1:200, 115-605-166, Jackson Immunoresearch) for 2 h at room temperature. After thorough washing in PBS, sections were counterstained, mounted, and coverslipped as above.

2.6. Quantification and analysis of immunostaining

Photomicrographs of all sections containing AP, NTS, LPBN, and CeA were taken at 20× magnification and a numeric aperture of 0.5, using a light microscope (Zeiss fluorescent microscope). The total number of Fos-positive cells and colocalization of CGRP/Fos were assessed automatically after thresholding all the images similarly in ImageJ by counting Fos-positive nuclei and counting the nuclei colocalized with CGRP neurons.

2.7. Experiments related to Figure 1: permanent and transient silencing of $CGRP^{LPBN}$ neurons through cre-dependent TeTxLC virally-mediated depletion and chemogenetic inhibition

2.7.1. LPBN viral infusion

An AAV carrying the Cre-dependent tetanus toxin light chain virus, ssAAV-8/2-hEF1α-dlox-FLAG_TeTxLC (rev)-dlox-WPRE-hGHp(A) (Physical titer: 4.2 × 10E12 vg/ml) (n = 11: n = 6 males, n = 5 females) or a control virus, ssAAV-8/2-hEF1α-dlox-EGFP(rev)-dlox-WPRE-bGHp(A) (Physical titer: 5.2 × 10E12 vg/ml) (n = 11: n = 5 males, n = 6 females) was injected directly in the LPBN of Calca Cre/+ mice. In a second cohort of mice, an AAV-carrying the Cre-dependent (inhibitory) hM4Di transgene, ssAAV-1/2-hSyn1-dlox-hM4D (Gi)_mCherry (rev)-dlox-WPRE-hGHp(A) (n = 16 males) (4.9×10^{12} vg/ml, 0.5 μl per site) or an AAV cre dependent mcherry transgene, ssAAV-1/2-hSyn1-dlox-mCherry (rev)-dlox-WPRE-hGHp(A) (5.4×10^{12} vg/ml, 0.5 μl per site, UZH Viral vector core) (n = 12 males) was injected in the LPBN of Calca Cre/+ mice.

The stereotaxic injection of the AAV was performed as previously described [22]. Briefly, mice were anesthetized with a mixture of ketamine (40 mg/kg in 0.9% NaCl s.c.; Ketanarkon, Streuli Pharma) and medetomidine hydrochloride (0.8 mg/kg in 0.9% NaCl s.c.; Medetor, Virbac, Glattbrugg, Switzerland). Before starting the surgery, antibiotics (Baytril: 10 mg/kg in 0.9% NaCl s.c.; Bayer, Leverkusen, Germany) were administered prophylactically. AAVs (0.5 μl per side) were injected bilaterally into the LPBN, at a rate of 100 nl/min, using the following coordinates: antero-posterior (AP), −4.9 mm; medio-lateral (ML), ±1.40; dorso-ventral (DV), 3.8 mm according to Paxinos and Watson [32], with NanoFil syringes 33 GA beveled (World Precision Instrument, Friedberg, Germany).

After the surgical procedures, mice were treated with an anti-inflammatory drug (Metacam 1.5 mg/kg s.c.; Boehringer Ingelheim, Biberach, Germany) and Revertor (3.5 mg/kg; Virbac), a selective α2 adrenergic receptor antagonist to reverse the sedative effects of medetomidine. Following surgery, animals were single-housed and treated for 3–5 days with antibiotics (Baytril/Enrofloxin, 10 mg/kg, SC) and anti-inflammatory drugs (see above). Mice were monitored daily and were left to recover for three weeks before starting the experiments.

2.7.2. Two-bottle test preference paradigm

The two-bottle test is a well-established learning and memory paradigm in rodents that is considered to be a special form of classical conditioning in which rodents, as well as many other species including humans, learn to associate a novel taste with malaise, and as a consequence avoid drinking fluid with this specific taste. To assess the ability of sCT and amylin to induce conditioned avoidance this paradigm was employed as described previously [33,34,35]. Briefly, mice (n = 22, n = 11/sex) were habituated to a water deprivation schedule for 7 days in which water access was given once daily for 90 min, beginning at the dark onset. Food was available ad libitum. Mice were randomized by sex and body weight and assigned to one of four experimental conditions for the training day: sCT (10 μg/kg, n = 6), amylin (500 μg/kg, n = 5), LiCl (84 mg/kg, positive control n = 5) or saline (negative control, n = 5). In the training days, mice have access to two bottles containing the same flavor of saccharin-sweetened Kool-Aid during the fluid access period (1.3 g Kool-Aid powder [for example cherry or grape, lime or orange, equally preferred by mice [36]], 0.5 g saccharin in 1 L tap water). Immediately after the fluid access period, mice were injected with their assigned drug or vehicle. Order of drug/vehicle exposure and paired flavors were counterbalanced. Each training day was followed by two days where tap water was available during the fluid access period (90 min). Two days after the second training day, mice were tested for expression of conditioned taste avoidance by giving them access to both flavors (one per bottle) and liquid intake was measured after the 90 min access period (bottle sides switched at 45 min to minimize side preference).

2.7.3. Sacrifice and brain processing

After a 12-hour fast in the light phase, mice were injected at dark onset with sCT (50 μg/kg i.p.) or vehicle. 90 min later animals were deeply anesthetized and transcardially perfused. Four series of 25 μm thick coronal sections containing the LPBN from bregma level −5.20 mm to − 5.34 mm [37], and CeA, from bregma level − 0.82 mm to −1.82 mm [37], were cut on a cryostat. Tissue was processed for Fos to determine the neural activation through the LPBN and the LPBN projection site, the CeA.

2.8. Experiments related to Figure 2: effects of CGRP KD in chow and HFD fed rats

2.8.1. LPBN viral injection

To site-specifically knockdown CGRP expression in the LPBN, an AAV encoding for 4 short hairpin RNA (shRNA) against CGRP mRNA (ssAAV-8/2-hSyn1-chl [4x (shrCGRP)]-EGFP-WPRE-SV40p(A)) (Suppl. Figure 7, Viral Vector Core, University of Zurich) was bilaterally infused

(6.6×10^{12} vg/ml, 1 ul/site, at a rate of 100 nl/min) into the LPBN under stereotactic surgery in 41 male rats (300–350 g). Forty control rats were injected with the AAV GFP control virus, ssAAV-8/2-hSyn1-chl [4x (shm/rNS)]-EGFP-WPRE-SV40p(A) (4.1×10^{12} vg/ml, 1 ul/site, at a rate of 100 nl/min). LPBN coordinates were as followed: anteroposterior (AP) −9.4 mm, mediolateral (ML) +/− 2.2 mm, dorsoventral (DV) 6.9 mm. After the surgery, rats were monitored daily and left to recover three weeks before starting the experiments.

2.8.2. Confirmation of CGRP gene knockdown

To validate the efficacy of the viral KD, operated rats (n = 17, n = 8/GFP control virus and n = 9/shrCGRP) were decapitated, and the brains were collected and stored at −80 °C until further processing. In the cryostat, micro punches of the LPBN were obtained using a 2 mm micropuncture (Soft Tissue Biopsy Punch, Zivic Instruments, USA). RNA was extracted and purified from each tissue punch according to the manufacturer's instructions (Z6111, Reliaprep, Promega, USA) and quantified using the spectrophotometer (NanoDrop, 2000; Thermo Fischer Scientific, USA). The extracted RNA was reverse transcribed to cDNA using the SensiFAST cDNA Synthesis Kit (BIO-65054, Bioline, UK). Fast quantitative real-time PCR using pre-designed CGRP Taqman probes (Rn01511353_g1, Applied Biosystems, USA) was performed. GAPDH (Rn01775763_g1, Applied Biosystems) was used as a housekeeping reference gene to quantify gene expression in the brain tissue.

2.8.3. Two-bottle test preference paradigm

The above-mentioned paradigm in mice was employed for rats (CGRP-KD experiment in lean animals). Animals were divided into four different treatment groups: sCT (5 ug/kg, n = 8), amylin (500 ug/kg, n = 8), LiCl (84 mg/kg, n = 8), or saline (n = 8), and the experiment was conducted as described above.

2.8.4. Glucose tolerance test

Food was removed 2 h prior to lights off and rats were gavaged at lights off, using a rat intra-gastric needle with 2 g/kg of D-glucose (0.5 g/mL). Sixteen rats were used for this experiment: eight control rats and eight $CGRP^{LPBN}$ KD rats. Blood was sampled from the tail prior to gavage (0) and at 15, 30, 60, 90, and 120 min post-gavage for glucose measurement (Glucometer: Breeze2, Bayer, Zurich, Switzerland).

2.8.5. Indirect calorimetry measurements

A 16-cage TSE PhenoMaster open-circuit indirect calorimetry system was used for the determination of O2 consumption and CO2 production (TSE Systems; Bad Homburg, Germany). Sixteen rats were used for this purpose: 8 control rats and 8 $CGRP^{LPBN}$ KD rats. The system was calibrated using precision calibration gases prior to each run. Room air was passed through each cage at a flow rate of 0.41 L/min. Every 20 min, cage air was sampled from each individual cage and analyzed for O2 and CO2. From these values, energy expenditure (EE) and respiratory exchange ratio (RER) were calculated based on equations from Weir [38]. To account for differences in body weight and body mass composition, EE data were corrected for individual lean body mass (LBM in g) and fat mass (FM in g) using the following equation: LBM + 0.2FM, as recommended by Even and Nadkarni [39,40]. Two days of baseline were measured and averaged. Then animals received sCT (5 ug/kg) that is known to increase EE [41].

2.8.6. Body composition

At the end of the study, body composition was measured in rats post-mortem by a magnetic resonance imaging (MRI) based approach to quantify total fat and lean mass. Rats were individually placed in a plastic holder, the holder was inserted into a tubular space in the EchoMRI (Echo Medical System, Houston, Texas, USA) and the scanning started. Scanning was repeated two times per animal and the results were delivered as numeric values ready to analyze.

2.8.7. Sacrifice and brain processing

After completion of the behavioral experiments, rats were fasted for 12 h during the light phase and at dark onset. They received an injection of amylin (50 μg/kg i.p.) or a vehicle. Ninety min later, animals were deeply anesthetized, perfused, and processed as above. Brains of LPBN (bregma level −8.72 mm to −10.04 mm) and CeA (bregma level −1.60 mm to −3.30 mm) were cut at the cryostat. Sections were immunostained for CGRP/Fos to verify the CGRP depletion in LPBN and neural activation through the LPBN and the LPBN projection site, the CeA.

2.9. Experiments related to Figure 3: comparison of amylin's and sCT's capacity to induce neuronal activation in AP, NTS, LPBN, and CeA

Male Sprague–Dawley rats (n = 22) weighing between 250 and 275 g at the time of arrival, were acclimated for 1 week. Rats were fasted for 12 h and at dark onset, and then received an i.p. injection of amylin (n = 8, 500 μg/kg) or sCT (n = 8, 5 μg/kg) or vehicle (n = 6) and 90 min later were perfused as described above. Four series of 25 μm thick coronal sections containing the AP (bregma level −13.68 mm to −14.08 mm) and the NTS (bregma level − 10.80 mm to −14.60 mm) LPBN and CeA were cut on a cryostat and stored at −20 °C as described before. Sections were processed for Fos and subsequently analyzed as described above.

2.10. Experiments related to Figure 4: evaluation of amylin and sCT effects on malaise

2.10.1. Evaluation of amylin and sCT potential aversive affective effects using the taste reactivity test

To assess disgust/aversive responses in non-vomiting rodent models, the taste reactivity (TR) test was employed [42,43]. The TR test measures affective reactions to food-related stimuli, quantifying affective reactions from hedonic and disgust/aversive categories, and by representing the conditioning dependent change in the display of taste stimulated hedonic to disgust/aversive reactions that result from associating a food stimulus with visceral malaise-inducing treatment [43]. Treatments that evoke visceral malaise (e.g., lithium chloride; GDF15), when associated with novel taste stimuli, alter the pattern of affective response from hedonic to disgust aversive. For example, food stimuli associated with negative consequences other than visceral malaise, such as peripheral pain or lactose malabsorption, reduce food consumption through a conditioned avoidance process but importantly do not result in affective aversive conditioned disgust/aversive responses [44,45]. Rats (n = 29) were anesthetized with ketamine (90 mg/kg; Midwest Veterinary Supply, Norristown, PA), xylazine (2.7 mg/kg; Anased, Shenandoah, IA) and acepromazine (0.64 mg/kg Midwest Veterinary Supply, Norristown, PA) followed post-surgically with Analgesia (2.0 mg/kg Loxicom; Midwest Veterinary Supply, Norristown, PA) and were implanted with bilateral intraoral (IO) cannula consisting of polyethylene (PE-100) tubing heat flared to hold a Teflon washer on the proximal end and press-fit with 19G stainless steel tubing on the distal end according to the protocol [43]. Briefly, each IO cannula was implanted lateral to the first maxillary molar and then anchored to the skull with a head cap made from four set screws and

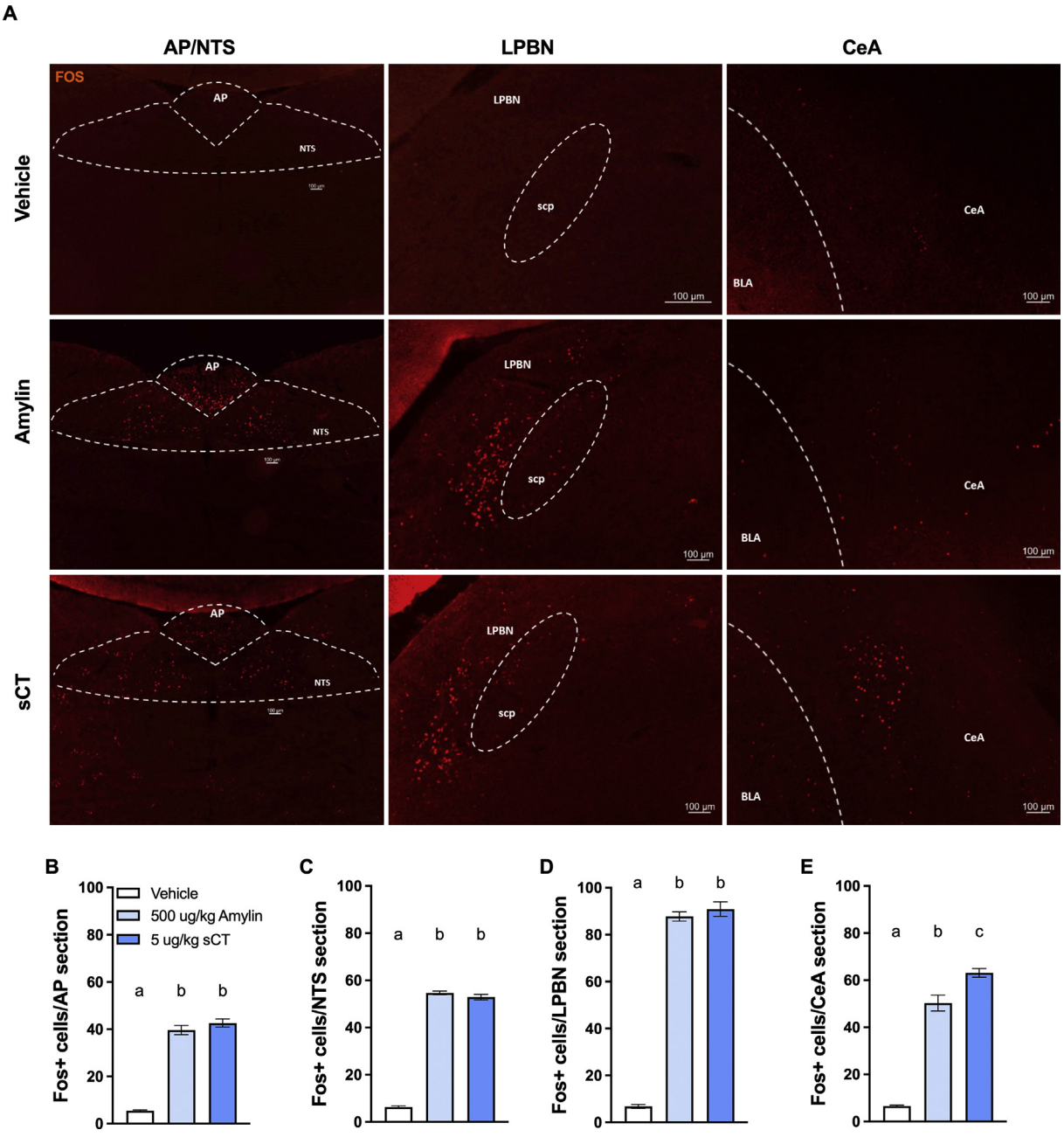

Figure 3: Amylin and sCT induce similar neuronal responses in AP, NTS and LPBN neurons but amylin-induced Fos is decreased in CeA neurons. (A) Representative images of Fos (red), after systemic acute administration of vehicle (0.9% NaCl, i.p, n = 6) or amylin (500 µg/kg, i.p., n = 8) or sCT (5 µg/kg, i.p., n = 8) in 12-hour fasted rats, in AP/NTS, LBPN and CeA. (B) Total Fos cells per AP section. (C) Total Fos cells per NTS section. (D) Total Fos cells per LPBN section. (E) Total Fos cells per CeA section. All data expressed as mean ± SEM. Data in (B–E) were analyzed using a one-way ANOVA test. [a,b, c] Data points with differing superscripts differ from each other at the $P < 0.05$ level.

dental acrylic. Postoperative antibiotic (Baytril/Enrofloxin, 10 mg/kg, s.c.) and analgesic (Meloxicam, 2 mg/kg, s.c.) were administered immediately after surgery and once daily for three days. Rats were given a limited amount of chow mash (50% powdered chow: 50% H_2O) after surgery and for at least two following days before ad libitum access to hard chow.

Saccharin (Acros Organics, Geel, Belgium, 0.15% w/v in distilled water) was used as a food stimulus in the taste reactivity test session. Rats were naive to the stimulus selected on the test day exposure. The i.p. drugs-food stimulus pairing was made as described below. Starting 3 days post-operatively until the start of the experiment, IO cannulas were flushed with water daily. A week prior to the experiment the 19G metal end of an IO cannula was attached to the infusion line and all rats were habituated to the test chamber for at least 5 min. The day before the start of the experiment, rats underwent a mock recording session. They were placed in the chamber, given 30 min to acclimate, and then infused with tap water for 30 s at the same rate (1 mL/min). Taste reactivity habituation and testing were conducted in a cylindrical chamber with clear Plexiglas walls and floor. A mirror was mounted at a 45° angle just below the clear chamber floor and a digital video camera (Toshiba Camileo H30 HD) was positioned facing the mirror on a tripod ~35 cm away. The

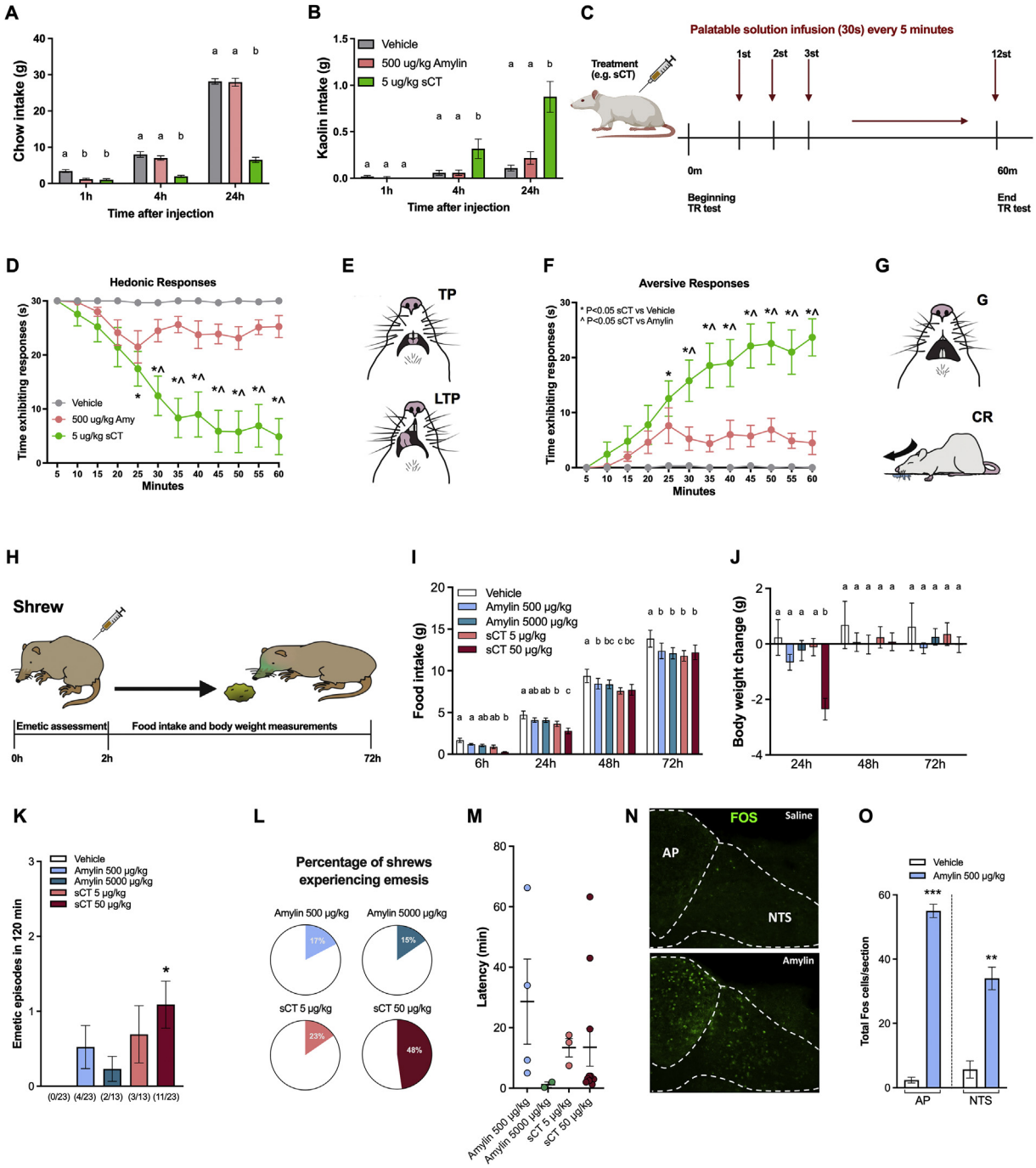

Figure 4: sCT, but not amylin, induces malaise. (A–B) Effects of systemically delivered vehicle (0.9% NaCl i.p, n = 12), amylin (500 µg/kg, i.p., n = 12) or sCT (5 µg/kg, i.p., n = 12) in 12-hour fasted rats on chow intake (A) and kaolin intake (B) in rats (n = 12). (C) Schematic representation of taste-stimulated affective responses associated with drug treatment (e.g. sCT) via a conditioned process. The palatable solution was infused for 30s every 5 min for a total of 60 min. During each infusion, affective responses were videotaped and later scored by an experimenter unaware of the treatment condition. Responses were categorized as hedonic or disgust/aversive and the total time spent displaying responses of both categories are graphed. (D) Hedonic responses expressed after sCT-palatable food association. (E) Examples of two hedonic responses: tongue protrusion (TP); lateral tongue protrusion (LTP). (F) Aversive responses expressed after sCT-palatable food association. (G) Examples of two disgust/aversive responses: gapes (G) and chin rubs (CR). (H) Schematic representation of the paradigm employed in shrews. (J) Effects of sCT (5 and 50 µg/kg), amylin (500 and 5000 µg/kg) or saline on cumulative food intake in shrews (n = 13). (I) Effects of sCT (5 and 50 µg/kg), amylin (500 and 5000 µg/kg) or saline on body weight in shrews (n = 13). (K) Number of single emetic episodes following saline, amylin (500 and 5000 µg/kg) or sCT (5 and 50 µg/kg) administration. (L) Percentage of shrews experiencing emesis after amylin (500 and 5000 µg/kg) or sCT (5 and 50 µg/kg) systemic delivery. (M) Latency to the first emetic episode in amylin and sCT treated animals that exhibited emesis. (N) Representative immunostainings of the AP/NTS region showing Fos response following saline and amylin (500 µl/kg) systemic treatment in shrews. (O) Quantification of Fos immunoreactive cells in the AP/NTS of shrews 2 h after saline or amylin (500 ug/kg, n = 3/group) injection. Data in (A–B), (D) and (F) were analyzed using a two-way ANOVA, followed by Sidak's post hoc tests. Data in (J–I) were analyzed using a two-way ANOVA, followed by Tukey's post hoc tests. Data in (K) were analyzed using a one-way ANOVA, followed by Tukey's post hoc tests. Data in (O) were analyzed using an unpaired t-test. *p < 0.05; **p < 0.01; ***p < 0.001. [a,b] Data points with differing superscripts differ from each other at the P < 0.05 level or less. See also Figs. S5 and S6.

PE-100 infusion line connected the rat's IO cannula to a 10-mL syringe secured to an infusion pump (Harvard Apparatus) that contained the food stimulus. This arrangement allowed the rats to move freely about the testing chamber.

On testing days, rats were injected intraperitoneally with the drugs (amylin 500 μg/kg, sCT 5 μg/kg or vehicle) and then connected to the infusion pump and habituated to the chamber for approximately 1–2 min before the infusion commenced. The experimenter activated the camera and tracked the animal ventral surface focusing on the oral-facial region. The animals were infused with the saccharin solution every 5 min for 30 s for 60 min (12 infusions in total).

In another cohort of animals (Suppl. Fig. 5), on testing days, rats were infused with the saccharin solution for 15 s over a 1 min period (4 infusions in total). After the last infusion rats were i.p. injected with the drugs (amylin 500 μg/kg, sCT 5 μg/kg or vehicle). After 3 days rats were infused with the saccharin solution to assess the behavioral response. Taste reactivity affective behavior analysis video files were viewed offline in slow motion as well as in real-time by a trained observer (H.J.G) who was blinded to the experiment.

2.10.2. Effects of acute amylin and sCT administration on kaolin and food intake

To assess nausea in non-vomiting rodent models, the pica behavior analysis was used [46,47]. Rats (n = 12) weighing ~250–265 g at arrival were individually housed in a hanging wire-bottomed cage with ad libitum access to chow diet (Purina Lab Diet 5001, St. Louis, Missouri) and tap water. Additionally, rats were exposed to kaolin for at least 5 days before measuring kaolin consumption in pica testing. Rats were fasted 2 h and then received i.p. injections at dark-onset of 500 μg/kg amylin, 5 μg/kg of sCT or saline. Kaolin intake and food intake were measured at 1, 4, and 24 h. Body weights were measured at 0 and 24 h.

2.10.3. Evaluation of food intake, body weight, emetic actions of amylin and sCT in shrews

Shrews (n = 23) were habituated to i.p. injections and to clear plastic observation chambers (23.5 × 15.25 × 17.8 cm) for two consecutive days prior to experimentation. Two hours before dark-onset, the animals were injected i.p. with sCT (5 and 50 μg/kg), amylin (500 and 5000 μg/kg), or saline, then video-recorded (Vixia HF-R62, Canon) for 120 min. After 120 min, the animals were returned to their cages. In a sub-group of animals (n = 13) food intake was measured at 6, 24, 48, and 72 h post-injection as previously described [48]. Body weights were taken at 0, 24, 48, and 72 h. Treatments occurred in a within-subject, counter-balanced design and were 7 days apart.

At the end of the experiment, a subgroup of animals (n = 10) was injected with the GLP-1R agonist Exendin-4 (Ex4, 30 μg/kg i.p.) or saline. Emetic episodes, food intake, and body weight were measured as described above. Treatments occurred in a within-subject, counter-balanced design and were 7 days apart.

2.10.4. Assessment of neuronal activation in the AP/NTS following amylin or saline treatments in shrews

Body weight-matched shrews (n = 3/group) received an i.p. injection of amylin (500 μg/kg) or saline just prior to dark onset. Food was removed to avoid feeding-related changes in Fos expression between groups. Two hours later, shrews were deeply anesthetized with i.p. triple cocktail of ketamine, xylazine and acepromazine (180 mg/kg, 5.4 mg/kg and 1.28 mg/kg; respectively) and transcardially perfused with 0.1 M PBS (Boston Bioproducts), followed by 4% PFA (in 0.1 M PBS, pH 7.4, Boston Bioproducts). Brains were removed and post-fixed in 4% PFA for 48 h and then stored in 25% sucrose for two days. Brains were subsequently frozen in cold hexane and stored at −20 °C until further processing. Thirty micrometer-thick frozen coronal sections containing the AP/NTS were cut on a cryostat (CM3050S, Leica Microsystem), collected, and stored in cryoprotectant (30% sucrose, 30% ethylene glycol, 1% polyvinyl-pyrrolidone-40, in 0.1 M PBS) at −20 °C until further processing. Immunohistochemistry was conducted according to the previously described procedure [48]. Briefly, free-floating sections were washed with 0.1 M PBS (3 × 8min), incubated in 0.1 M PBS containing 0.3% Triton X-100 (PBST) and 5% normal donkey serum (NDS) for 1 h, followed by overnight incubation with rabbit anti-Fos antibody (1:1000 in PBST; 2250; Cell Signaling). After washing (3 × 8min) with 0.1 M PBS sections were incubated with the secondary antibody donkey anti-rabbit Alexa Fluor 488 (1:500 in 5% NDS PBST; Jackson Immuno Research Laboratories) for 2 h at room temperature. After final washing (3 × 8min in 0.1 M PBS) the sections were mounted onto glass slides (Superfrost Plus, VWR) and coverslipped with Fluorogel (Electron Microscopy Sciences). Fos-positive neurons spanning the AP/NTS were visualized (20x; Nikon 80i, NIS Elements AR 3.0) and quantified (FIJI software) using fluorescence microscopy. A total of 4 AP/NTS sections per animal were used to quantify the number of Fos labeled cells in the AP and NTS at the level of the caudal medial DVC (200 and 250 μm rostral to the obex, and medial DVC, similarly as previously described [49] by an experimenter blinded to the treatment.

2.11. Quantification and statistical analysis

Data are reported as mean ± standard error of the mean (SEM). Statistical analyses of physiologic data were performed with Prism software (version 8). For all statistical tests, a p-value <0.05 was considered statistically significant. Information on replicates and significance are reported in the figure legends.

In the experiment related to Figure 1, baseline and post-treatment food intake, meal patterns, body weight, and brain study data were analyzed using a two-way ANOVA followed by Sidak's post hoc tests. CTA data were analyzed using a one-way ANOVA.

In the experiment related to Figure 2, qPCR data were analyzed with a student t-test. Baseline and post-treatment food intake, meal patterns, body weight, lean and fat mass, RER and EE, and brain study data were analyzed using a two-way ANOVA followed by Sidak's post hoc tests. CTA data were analyzed using a one-way ANOVA.

In an experiment related to Figure 3, Fos quantification was analyzed using a one-way ANOVA.

In the experiment related to Figure 4, the chow and kaolin intake data and the TR test data were analyzed using a two-way ANOVA followed by Sidak's *post hoc* tests (serial method) or with one-way ANOVA (standard method). Food intake and body weight changes in shrews were analyzed using two-way ANOVAs followed by Tukey's post-hoc tests. Comparisons between different proportions of shrews experiencing emesis under the different treatment conditions (i.e. occurrence) were made using Fisher's exact test. The total number of emetic episodes was analyzed using one-way ANOVA followed by Tukey's *post-hoc* test. For immunohistochemistry, statistical comparisons were performed using unpaired t-tests.

3. RESULTS

3.1. Permanent and temporary inhibition of $CGRP^{LPBN}$ neurons blocked sCT but not amylin anorectic effect

In a previous study, we revealed that about 1/3 of amylin-activated neurons in the rat LPBN are CGRP-ergic [9]. To more deeply

evaluate the involvement of CGRP-ergic signaling in mediating amylin's and sCT's effects, $CGRP^{LPBN}$ neurons in $Calca^{Cre/+}$ transgenic mice (Calca is the gene that encodes CGRP, and these mice express the Cre recombinase at the Calca locus) were permanently silenced with an AAV encoding for tetanus toxin (TeTxLC) to block release of neurochemicals (Figure 1 A). Under baseline conditions, there were no differences in food intake (Figure 1 B) and body weight (Figure 1 C-D). Importantly, $CGRP^{LPBN}$ neurons silencing reduced sCT (10 μg/kg, i.p.), but not amylin (50 μg/kg and 500 μg/kg, i.p.) acute anorectic effect at 1 h and 2 h (Figure 1 E-J). In comparison, amylin and sCT were able to decrease eating in control rats (Figure 1 E, G, H, I). $CGRP^{LPBN}$ neurons silenced animals (TeTxLC) were resistant to the anorectic effect of LiCl (Figure 1 K), functionality validating the effectiveness of the experimental design [22]. No significant difference between silenced and non-silenced $CGRP^{LPBN}$ animals was observed in the meal pattern analysis (Suppl. Figure 1).

To further investigate the role of CGRP neurons in the mediation of other behavioral components of feeding behaviors that could be affected by amylin and sCT, we tested their effects on conditioned taste avoidance and compared results to the positive control LiCl (Figure 1 L-N). The conditioned avoidance test showed that similarly to LiCl, sCT administration reduced preference of the associated taste stimulus and thereby conditioned a taste avoidance in the control animals (Figure 1 M). In contrast, no conditioned alteration in taste preference was observed in control animals treated with amylin (Figure 1 M), indicating a difference between amylin and sCT effect. Importantly, silencing of $CGRP^{LPBN}$ neurons blocked the ability of sCT as well as LiCl to condition a taste avoidance (Figure 1 N), pointing out the necessary role of $CGRP^{LPBN}$ neurons in conveying this effect.

Next, we examined whether $CGRP^{LPBN}$ neuron silencing alters sCT's ability to activate LPBN and CeA neurons (Figure 1 O-T). The total number of the $CGRP^{LPBN}$ neurons was not different between the control and the TeTxLC group (Figure 1 O). The TeTxLC inhibition reduced the number of sCT-activated LPBN and CeA neurons by 16% and 56%, respectively, compared to control sCT-treated mice (Figure 1 P-T). In the control group, 45% of sCT activated LPBN neurons were CGRP neurons (Figure 1 Q), and $CGRP^{LPBN}$ neurons silencing resulted in a 59% reduction of the number of sCT activated $CGRP^{LPBN}$ neurons (Figure 1 Q). These data are consistent with the lack of an inhibitory feeding response in the TeTxLC group after sCT treatment (Figure 1 H—I).

To confirm the TetTox treatment results, a complementary inhibitory Designer Receptors Exclusively Activated by Designer Drugs (DREADD)-based chemogenetic technique was used in combination with the $Calca^{Cre/+}$ transgenic mice (Suppl. Figure 2 A). The behavioral results of the CNO-mediated temporal inhibition of $CGRP^{LPBN}$ neurons via hM4Di-activation were consistent with the results of the permanent inhibition (Suppl. Figure 2A—I). Furthermore, immunohistological analyses also yielded similar outcomes: the lack of an inhibitory feeding response following sCT was also reflected by a 35% overall reduction of neuronal activation in the LPBN of hM4Di mice treated with CNO/sCT compared to the sCT-treated control mice (Suppl. Figure 2 J-K), and by a 62% reduction in the number of activated $CGRP^{LPBN}$ neurons (Suppl. Figure 2 M-L). Altogether, these two sets of complementary behavioral and neuro-physiological experiments provide strong evidence that silencing of $CGRP^{LPBN}$ neurons attenuates sCT but not amylin effect on food intake and neuronal activation.

3.2. CGRP release from $CGRP^{LPBN}$ neurons is not required for amylin's and sCT's hypophagic effects in lean and obese rats

To investigate the specific role of CGRP as a neuropeptide released from $CGRP^{LPBN}$ neurons in mediating amylin's and sCT's effects, CGRP expression was knocked down (KD) in LPBN neurons. This was achieved via an adeno-associated virus that encodes for short hairpin RNA against CGRP mRNA in rats (Figure 2 A). Gene expression analysis in a separate small cohort of animals showed that CGRP expression was reduced by 65% (Figure 2 B). $CGRP^{LPBN}$ KD did not alter body weight (Figure 2 C), baseline food intake (Figure 2 D) and glucose tolerance (Figure 2 E) prior to any pharmacological treatment, nor did not affect the ability of sCT (5 μg/kg) or amylin (50 μg/kg, 500 μg/kg) to induce hypophagia (Figure 2 F—H) or to reduce meal size (Suppl. Figure 3).

Next, the depletion of CGRP from LPBN neurons on conditioned avoidance following amylin, sCT or LiCl injections was tested. In line with our murine data (Figure 1 M), sCT and LiCl, but not amylin, conditioned avoidance in control rats (Figure 2 I). Interestingly, sCT-induced conditioned taste avoidance was maintained and similar to LiCl in CGRP KD rats (Figure 2 J) suggesting that CGRP as a neuropeptide is not necessary to elicit conditioned avoidance after sCT treatment.

In addition to confirming the injection accuracy and spreading of the virus within the LPBN (Figure 2 P), we examined whether $CGRP^{LPBN}$ KD attenuated amylin's ability to activate LPBN and CeA neurons (Figure 2 K-R). Notably, CGRP immunoreactivity in the $CGRP^{LPBN}$ KD group was reduced by ~50%, complementing the mRNA expression data and further confirming the ability of the AAV KD virus to reduce CGRP expression at the protein level (Figure 2 M). In line with our previous results, amylin increased LPBN neural activation in control rats (Figure 2 L), specifically, 32% of activated neurons were CGRP neurons (Figure 2 N). Even though the number of $CGRP^{LPBN}$ activated neurons was decreased by 50% in the $CGRP^{LPBN}$ KD rats compared to controls (Figure 2 N), the total number of amylin-induced Fos neurons was similar in both groups (Figure 2 L). Indeed, the majority of amylin-activated neurons in the LPBN were not CGRP + as there was also no difference in the number of non-CGRP activated neurons in both groups (Figure 2 O). We did however notice a significant 25% reduction in the number of amylin activated neurons in the CeA in the KD group (Figure 2Q—R). Altogether these results further confirm that CGRP released from $CGRP^{LPBN}$ neurons does not play a major role in the mediation of amylin-induced eating behaviors.

Lastly, to test whether impaired CGRP signaling could enhance hyperphagia and obesity under HFD conditions, we performed a similar set of experiments in a separate cohort of animals maintained on HFD for 8 weeks after viral injection (Suppl. Figure 4). CGRP knockdown in LPBN significantly increased body weight by +12% compared to the control group; however, no other metabolic alterations were observed. Overall, these data suggest that $CGRP^{LPBN}$ signaling is not necessary for physiological satiation induced by amylin but may have a role in long-term body weight control under obesogenic conditions.

3.3. Amylin and sCT induce similar neuronal responses in AP, NTS and LPBN neurons but amylin-induced Fos is decreased in CeA neurons

Both amylin and sCT are known to activate AP/NTS neurons that project to the LPBN and LPBN neurons directly project to neurons located in the CeA [7,12]. However, a direct comparison between sCT- and amylin-induced neuronal activation in the LPBN and CeA has never been performed. We compared the highest amylin (500 μg/kg) and sCT (5 μg/kg) dose used in rats as they both comparably decreased 1-hour food intake. Fos expression in AP/NTS (Figure 3 B—C) and LPBN (Figure 3 D) did not differ between amylin and sCT. There was, however, a higher number (+25%) of Fos positive cells in CeA (Figure 3 E) after sCT compared to amylin. Together, these results suggest that the recruitment and activation of a larger percentage of $CGRP^{LPBN}$ neurons

following sCT may likely be the reason for the greater number of Fos positive cells within the CeA (compared to amylin).

3.4. sCT, but not amylin, induces pica and affective taste aversion in rats and emesis in musk shrews

Building upon the conditioned taste avoidance results, we investigated whether sCT and amylin would induce behaviors indicative of malaise/sickness that could contribute to their hypophagic effects. First, we assessed nausea in rats using the pica test (i.e. kaolin consumption) as a proxy of nausea in non-vomiting species like laboratory rodents [46,47]. Despite the similar suppression of food intake at 1 h for sCT and amylin (5 μg/kg and 500 μg/kg; respectively) (Figure 4 A), only sCT significantly increased kaolin consumption at 4 h and 24 h (Figure 4 B).

We expanded our analysis by investigating whether amylin and sCT could condition an affective disgust—aversive reaction to a novel palatable food (i.e., saccharin) that could explain the acute reduction in feeding and, separately, whether sCT conditions a disgust/aversive reaction to food whose effect persists beyond the period of drug action to reduce food intake in the longer term. For this purpose, taste reactivity test paradigms were employed in rats implanted with an intraoral cannula that enable the direct oral infusion of taste stimuli, to assess changes in the pattern of stereotyped, oral-facial responses elicited by food stimuli [43]. Only treatments that induce an aversive visceral state (e.g., LiCl, GDF15) have been shown to produce conditioned affective aversive responses to food [35,45].

In one paradigm selected for assessing the rapid formation of taste aversion after LiCl administration in a single session following amylin (500 μg/kg), sCT (5 μg/kg) or vehicle, rats received orally delivered, 1-min infusions of saccharin every 5 min for 60 min and the elicited affective reactions were video recorded and subsequently scored by an experimenter blinded to treatment [42]. The effects of the sCT injection that were associated repeatedly with saccharin taste infusion showed that the taste-driven affective response changed from hedonic to disgust/aversive over time via a conditioning process. Following sCT, time spent displaying hedonic responses decreased significantly (Figure 4 E-F) while time spent displaying disgust/aversive responses increased significantly (Figure 4 G-H) compared to vehicle-treated rats. Importantly, in amylin-treated rats, no such difference in the time exhibiting hedonic (Figure 4 D) and aversive (Figure 4 F) responses, compared to the vehicle-treated rats was observed; amylin associated taste elicited hedonic responses throughout the entire test period.

To evaluate whether the aversive conditioned affective reactions following sCT persisted beyond the acute period of the drug administration, rats' affective reactions to the paired taste reactions were reassessed 3 days after treatment administration (either amylin 500 μg/kg or sCTs 5 μg/kg or vehicle) (Suppl. Figure 5 A). After sCT treatment, but not amylin, the rats displayed a significant decrease of hedonic reactions (Suppl. Figure 5 B) and an increase of aversive responses (Suppl. Figure 5 C).

Lastly, we assessed the emetogenic and anorectic profile of both amylin and sCT in musk shrews (*S. murinus*), a small mammal capable of emesis. The musk shrew is an established preclinical model for the study of emesis, as it shares an emetic profile similar to humans following chemotherapy and anti-obesity medications [49,50,51,52,53]. In line with previous reports in rodents, systemic administration of sCT (5 and 50 μg/kg i.p.) in shrews produced an hypophagic response in a dose-dependent fashion, leading to significant body weight loss for the highest dose tested (Figure 4 I-J). Only a modest, yet significant reduction in food intake occurred following both amylin treatments (500 and 5000 μg/kg i.p.) (Figure 4 I). Notably, sCT dose-dependently induced emesis while amylin did not (Figure 4 K). Approximately half of the shrews displayed emesis upon administration of the highest sCT dose tested (Figure 4 L). In contrast to the emetic responses observed after the high dose of sCT, both the prevalence and the number of emetic episodes following amylin were lower and did not significantly differ from saline-treated animals (Figure 4 K-L). In general, all doses of amylin and sCT triggered emesis within minutes after administration in the shrews experiencing emesis (Figure 4 M).

As a positive control, a subgroup of shrews was also injected with the GLP-1R agonist Exendin-4 (Ex4, 30 μg/kg i.p.). Similar to what has been previously demonstrated [48,54], systemic administration of Ex4 produced a hypophagic and body weight loss response that was comparable to the highest dose of sCT. Indeed, Ex4 induced a ~77% decrease in food intake at 6 h compared to a ~83% reduction following sCT (Suppl. Figure 6 A-B). In contrast, both the prevalence (80%) and the number of emetic episodes (8.7 ± 3.8) following Ex4 treatment were higher compared to sCT (Suppl. Figure 6 C). Thus, despite inducing comparable short-term anorectic responses, the emetogenic potential of sCT seems to be lower than Ex4 in this model. Importantly, amylin (500 μg/kg i.p.) induced a robust neuronal activation (i.e. Fos) in the AP and NTS 2 h after administration in shrews (Figure 4 O), confirming the engagement of the hindbrain by amylin in this model, thus excluding the hypothesis that absence of emesis was due to a lack of activity at the shrew AMY receptor.

4. DISCUSSION

In this study, we investigated the effects of amylin and sCT on food intake, conditioned avoidance, conditioned affective aversion, nausea, and emesis. We here present data that distinguish between behavioral responses and neuronal pathways involved in mediating the actions of amylin and sCT in LPBN and CeA. Our studies support the conclusion that $CGRP^{LPBN}$ neurons mediate sCT's effects on food intake and conditioned avoidance, while the inhibition of these neurons does not alter amylin-induced anorexia nor body weight regulation. As previously reported [55], sCT induced conditioned taste avoidance and amylin did not [56,57,58,59]. sCT's ability to induce avoidance is not blocked in CTR^{NTS} KD animals [55], consistent with our recent work in which no sCT binding was detected in the NTS [60].

We observed that amylin activates largely non-CGRP expressing neurons within the LPBN neurons, whose activation is not associated with conditioned avoidance. Moreover, $CGRP^{LPBN}$ neurons ablation did not decrease amylin anorectic response. Together, this suggests that the mild CGRP neuronal activation after amylin treatment as we and others have previously reported [9,22], is not necessary to elicit a behavioral response. Importantly, the phenotype of these non-CGRP activated LPBN neurons is unknown and their elucidation should deepen our understanding of amylin neurocircuitry and how it differs from sCT signaling.

We previously observed that rats with chemically-ablated noradrenaline neurons in the LPBN exhibited a reduced response to amylin and sCT, and also a reduced amylin-induced Fos response in CGRP and non-$CGRP^{LPBN}$ neurons [9]. Here, we observed that knocking-down *cgrp* mRNA expression in the LPBN, thus reducing the amount of CGRP neuropeptide produced by CGRP neurons, had no effect in mediating both amylin's and sCT's anorectic effect and conditioned taste avoidance behavior was still present after sCT application. While $CGRP^{LPBN}$ neurons are required to mediate sCT's and LiCl's anorectic and conditioned avoidance effect, it is important to consider that these neurons, in addition to CGRP, also express tachykinins and glutamate [23], neurotransmitters that play an important role in the central

mediation of nausea/emesis [61]. Tachykinin neurokinin receptor 1 (NK1R) antagonist, e.g. Aprepitant [62,63,64,65,66], has been developed and successfully employed to mitigate nausea and emesis in different medical fields (e.g. oncology). It is therefore likely that LPBN → CeA tachykinins and/or glutamate signaling, rather than CGRP itself, are the primarily neurotransmitters involved in mediating sCT's anorectic effects.

Our immunohistochemical study showed that sCT treatment produced a greater number of CeA neurons to be activated, relative to amylin. Within the CeA, different neuronal populations can be found. Of particular interest in this context is the subpopulation of neurons that express the marker protein kinase C-delta (PKCδ). Recent studies have shown that PKCδ+ neurons are required for the food intake suppression of diverse anorectic/aversive stimuli, such as GDF15 and LiCl [67,68]. Though the involvement of PKCδ in the mediation of sCT has not yet been investigated in the current study, one can hypothesize that sCT also activates these neurons to mediate anorexia and malaise.

Importantly, this study points out that sCT, but not amylin, induces affective aversion, nausea and emesis. Our results highlight that sCT induces a visceral malaise state marked by pica behavior that reduces food intake during the acute period of pharmacological action exerting the anorectic action. This corroborates previously published studies showing that a single low dose of amylin administered intraperitoneally (i.p., 100 μg/kg) or centrally (100 pmol, 3rd-ventricule), did not condition avoidance or trigger pica behavior in rats [56,57,58,59]. From these data, we conclude that anorexia and body weight loss produced by sCT treatment is mediated, at least in part, by inducing an aversive state [9,16,41,69].

Applying taste reactivity methods enabled direct measurement of conditioned affective taste responses. Repeated presentation of novel taste with the effects of sCT injection conditioned an affective taste aversion comprised of increased numbers of aversive affective reactions and decreased occurrences of hedonic responses to the presentation of the sCT associated taste. Our results in Figure 4 show that the expression of the conditioned affective response emerged at 25–30 min after drug administration and the magnitude of the shift in affective response, increased in magnitude over the remaining 30–35 min of the 60 min test. This is consistent with the data of Spector et al. [42], who first applied this paradigm to assess the rapid formation of condition affective response. They showed in a control experiment that delaying the presentation of the first taste infusion following LiCl injection by 20 min also delayed the appearance of the transition of affective response from hedonic to aversive by an additional 20–30 min. Importantly, those data support the view that a conditioned associative process mediates the observed affective response change [42]. The emergence of a shift in affective response through conditioning explains the similar profile of affective responses for taste associated with amylin and sCT during the saccharin infusions occurring within the first 20–25 min. The conditioned affective aversive response to sCT persisted beyond the acute action of the drug and thereby extended its anorectic action to the longer-term via conditioning.

We also report that exogenous administration of sCT causes emesis in musk shrews. In this model, sCT caused emesis within minutes of injection, as well as significant anorexia and body weight loss, the latter of which is consistent with previously published work in rodents from our lab and others [9,16,41,69]. We here demonstrated the emetogenic properties of sCT and the lack of thereof of amylin in a pre-clinical model. Such results, in a non-rodent mammalian species, further corroborate our conditioned avoidance, taste reactivity and pica results in rats and strengthen our initial hypothesis that sCT-induced anorexia could be driven, in part, by malaise. Conversely, both doses of amylin tested in shrews failed to induce emesis, despite significantly reducing food intake. The lack of emesis occurring following both tested doses of amylin, nicely corroborates the results obtained in rodents. Furthermore, amylin induces a strong Fos expression within the AP and NTS of the shrew, providing the first immunohistological evidence of the engagement of the hindbrain by amylin in this model, and excluding the hypothesis of lack of activity at the shrew AMY receptor as the reason for the absence of emesis in this model.

The incidence and magnitude of nausea/emesis observed in shrews and rodents is in line with clinical data on its use as an analgesic and treatment for osteoporosis. Indeed, clinical studies show sCT being mildly emetic with ∼10–20% of patients experiencing moderate to low adverse events of gastro-intestinal origin [70,71]. Additionally, combining the novel AMY/CTR agonist cagrilintide with the GLP-1R agonist semaglutide, yielded superior body weight loss, when compared to semaglutide alone, but it also increases the occurrence of gastric adverse events [72].

It is worth mentioning here that the magnitude and occurrence of the emetic responses and pica behavior were significantly lower compared to doses of E×4 that lead to similar reductions in food intake. This was expected given the wealth of literature reporting nausea and emesis as the principal side effects of existing GLP-1 therapeutics [73] and top reasons for treatment discontinuation [74]. Whether it is possible to dissociate the hypophagic and body weight lowering effects of sCT from malaise in pre-clinical and clinical settings remains a venue for future investigations.

5. CONCLUSION AND CLINICAL RELEVANCE

Obesity is a major health problem worldwide and it is estimated that, by the year 2030, 38% of the world's adult population will be overweight and another 20% obese [75]. Current options to treat obesity are limited with most patients quickly regaining about 30–50% of their lost weight upon lifestyle modifications only (i.e. diet and exercise) [76,77]. Hormonal pharmacological therapies represent a valuable strategy to induce and maintain weight loss. Amylin analogs (e.g., pramlintide and cagrilintide) alone or in combination with other drugs (e.g., semaglutide) are promising treatments for obesity [17,72,78,79]. This study deciphers the different mechanisms of amylin's and sCT's action, giving important insights for the generation of AMY receptor agonist-based anti-obesity therapeutics, with reduced incidence and severity of nausea and emesis, thus improving patient compliance and quality of life.

5.1. Limitation of the study

In this study, amylin and sCT were only evaluated in an acute experimental design. Future studies should evaluate the effect of chronic administration of amylin or sCT on hypophagia and malaise in emetic and non-emetic species. In this study, we did not assess whether the inhibition of $CGRP^{LPBN}$ neuronal activation would block aversion, nausea, and emesis. This was not possible because the rats and shrews used to evaluate malaise do not have the readily available genetic tools (i.e., genetic-based targeting approaches to reduce $CGRP^{LPBN}$ neuron signaling) that are available in mice.

RESOURCE AVAILABILITY

Lead contact and material availability

This study did not generate new unique reagents. Further information and requests for resources and reagents should be directed to and will be fulfilled by the Lead Contact, Christelle Le Foll (christelle.lefoll@uzh.

ch) and Thomas Lutz (tomlutz@vetphys.uzh.ch). Mouse lines or AAVs generated by this study will be available upon request.

Data and code availability

The published article includes all data generated or analyzed during this study. No code was used or generated in this study.

AUTHOR CONTRIBUTIONS

Conceptualization, L.B., H. J. G., T.B., C.L.F. and T.A.L.; Methodology, L.B. and C.L.F.; Investigation, L.B.,T.B., M.Y.G., P.K., C.P. S.A.D.; Writing — Original Draft, L.B.; Writing — Review & Editing, L.B, T.B, H.J.G., B.C.D.J., C.L.F and T.A.L Resources, T.A.L., H.J.G., B.C.D.J.; Funding Acquisition, T.A.L., H.J.G., B.C.D.J., T.B.

ACKNOWLEDGMENTS

This work was funded by the Swiss National Science Foundation (SNF 31003 A_175458 to TAL), (P400PB 186728 to TB) and by the National Institutes of Health (Grants DK112812 (to BCDJ), and DK021397 (to HJG). We would like to thank Pr. Richard Palmiter (University of Washington, WA) for providing us with the Calca-cre mouse breeders. We would like to acknowledge the technical contributions of Jean-Charles Paterna of the Viral Vector Facility, University of Zurich; the Center for Microscopy and Image Analysis, University of Zurich; Petra Seebeck of the Zurich Integrative Rodent Physiology (ZIRP), and Charles Daniel Furst, Department of Bio-behavioral Health Sciences, University of Pennsylvania.
We also thank the technical assistance of Janine Schlaepfer, Marissa Schraner, Salome Gamakharia and Bernd Coester (all UZH).

CONFLICT OF INTEREST

L.B., M.Y.G., P.K., C.P., S.A.D., H.J.G., C.L.F. and T.A.L. have no conflicts to declare. T.A.L. received research funding from Novo Nordisk and Boehringer not supporting these studies. B.C.D.J. received research funding from Eli Lilly & Co. not supporting these studies. H.J.G received research funding from Pfizer Inc, not used to support these studies. T.B., and B.C.D.J. are owners of Cantius Therapeutics, LLC that pursues biological work unrelated to the current study.

APPENDIX A. SUPPLEMENTARY DATA

Supplementary data to this article can be found online at https://doi.org/10.1016/j.molmet.2022.101444.

REFERENCES

[1] Hay, D.L., Chen, S., Lutz, T.A., Parkes, D.G., Roth, J.D., 2015. Amylin: pharmacology, Physiology, and clinical potential. Pharmacological Reviews 67(3):564—600. https://doi.org/10.1124/pr.115.010629.

[2] Riediger, T., Zuend, D., Becskei, C., Lutz, T.A., 2004. The anorectic hormone amylin contributes to feeding-related changes of neuronal activity in key structures of the gut-brain axis. American Journal of Physiology - Regulatory, Integrative and Comparative Physiology 286(1):R114—R122. https://doi.org/10.1152/ajpregu.00333.2003.

[3] McLatchie, L.M., Fraser, N.J., Main, M.J., Wise, A., Brown, J., Thompson, N., et al., 1998. RAMPS regulate the transport and ligand specificity of the calcitonin- receptor-like receptor. Nature 393(6683):333—339. https://doi.org/10.1038/30666.

[4] Qi, T., Christopoulos, G., Bailey, R.J., Christopoulos, A., Sexton, P.M., Hay, D.L., 2008. Identification of N-terminal receptor activity-modifying protein residues important for calcitonin gene-related peptide, adrenomedullin, and amylin receptor function. Molecular Pharmacology 74(4):1059—1071. https://doi.org/10.1124/mol.108.047142.

[5] Liberini, C.G., Boyle, C.N., Cifani, C., Venniro, M., Hope, B.T., Lutz, T.A., 2016. Amylin receptor components and the leptin receptor are co-expressed in single rat area postrema neurons. European Journal of Neuroscience 43(5):653—661. https://doi.org/10.1111/ejn.13163.

[6] Hilton, J.M., Chai, S.Y., Sexton, P.M., 1995. In vitro autoradiographic localization of the calcitonin receptor isoforms, C1a and C1b, in rat brain. Neuroscience 69(4):1223—1237. https://doi.org/10.1016/0306-4522(95)00322-A.

[7] Becskei, C., Grabler, V., Edwards, G.L., Riediger, T., Lutz, T.A., 2007. Lesion of the lateral parabrachial nucleus attenuates the anorectic effect of peripheral amylin and CCK. Brain Research 1162:76—84. https://doi.org/10.1016/j.brainres.2007.06.016. S0006-8993(07)01369-8 [pii].

[8] Lutz, T.A., Senn, M., Althaus, J., Del Prete, E., Ehrensperger, F., Scharrer, E., 1998. Lesion of the area postrema/nucleus of the solitary tract (AP/NTS) attenuates the anorectic effects of amylin and calcitonin gene-related peptide (CGRP) in rats. Peptides 19(2):309—317. https://doi.org/10.1016/S0196-9781(97)00292-1.

[9] Boccia, L., Le Foll, C., Lutz, T.A., 2020. Noradrenaline signaling in the LPBN mediates amylin's and salmon calcitonin's hypophagic effect in male rats. Federation of American Societies for Experimental Biology Journal 34(11):15448—15461. https://doi.org/10.1096/fj.202001456RRR.

[10] Mollet, A., Gilg, S., Riediger, T., Lutz, T.A., 2004. Infusion of the amylin antagonist AC 187 into the area postrema increases food intake in rats. Physiology & Behavior 81(1):149—155. https://doi.org/10.1016/j.physbeh.2004.01.006.

[11] Rowland, N.E., Crews, E.C., Gentry, R.M., 1997. Comparison of Fos induced in rat brain by GLP-1 and amylin. Regulatory Peptides. https://doi.org/10.1016/S0167-0115(97)01034-3.

[12] Boccia, L., Gamakharia, S., Coester, B., Whiting, L., Lutz, T.A., Le Foll, C., 2020. Amylin brain circuitry. Peptides, 170366. https://doi.org/10.1016/j.peptides.2020.170366.

[13] Lee, S.-M., Hay, D.L., Pioszak, A.A., 2016. Calcitonin and amylin receptor peptide interaction mechanisms: insights into peptide-binding modes and allosteric modulation of the calcitonin receptor by receptor activity-modifying proteins. Journal of Biological Chemistry 291(16):8686—8700. https://doi.org/10.1074/jbc.M115.713628.

[14] Buclin, T., Rochat, M.C., Burckhardt, P., Azria, M., Attinger, M., 2002. Bioavailability and biological efficacy of a new oral formulation of salmon calcitonin in healthy volunteers. Journal of Bone and Mineral Research 17(8):1478—1485. https://doi.org/10.1359/jbmr.2002.17.8.1478.

[15] Hilton, J.M., Dowton, M., Houssami, S., Sexton, P.M., 2000. Identification of key components in the irreversibility of salmon calcitonin binding to calcitonin receptors. Journal of Endocrinology 166(1):213—226. https://doi.org/10.1677/joe.0.1660213.

[16] Andreassen, K.V., Hjuler, S.T., Furness, S.G., Sexton, P.M., Christopoulos, A., Nosjean, O., et al., 2014. Prolonged calcitonin receptor signaling by salmon, but not human calcitonin, reveals ligand bias. PLoS One 9(3). https://doi.org/10.1371/journal.pone.0092042.

[17] Fletcher, M.M., Keov, P., Truong, T.T., Mennen, G., Hick, C.A., Zhao, P., et al., 2021. AM833 is a novel agonist of calcitonin family G protein—coupled receptors: pharmacological comparison with six selective and nonselective agonists. Journal of Pharmacology and Experimental Therapeutics 377(3):417—440. https://doi.org/10.1124/jpet.121.000567.

[18] Herbert, H., Moga, M.M., Saper, C.B., 1990. Connections of the parabrachial nucleus with the nucleus of the solitary tract and the medullary reticular formation in the rat. Journal of Comparative Neurology 293(4):540—580. https://doi.org/10.1002/cne.902930404.

[19] Beckstead, R.M., Morse, J.R., Norgren, R., 1980. The nucleus of the solitary tract in the monkey: projections to the thalamus and brain stem nuclei. Journal of Comparative Neurology. https://doi.org/10.1002/cne.901900205.

[20] Chiang, M.C., Bowen, A., Schier, L.A., Tupone, D., Uddin, O., Heinricher, M.M., 2019. Parabrachial complex: a hub for pain and aversion. Journal of Neuroscience 39(42):8225–8230. https://doi.org/10.1523/JNEUROSCI.1162-19.2019.

[21] Campos, C.A., Bowen, A.J., Schwartz, M.W., Palmiter, R.D., 2016. Parabrachial CGRP neurons control meal termination. Cell Metabolism 23(5):811–820. https://doi.org/10.1016/j.cmet.2016.04.006.

[22] Carter, M.E., Soden, M.E., Zweifel, L.S., Palmiter, R.D., 2013. Genetic identification of a neural circuit that suppresses appetite. Nature 503(7474):111–114. https://doi.org/10.1038/nature12596.

[23] Palmiter, R.D., 2018. The parabrachial nucleus: CGRP neurons function as a general alarm. Trends in Neurosciences, 280–293. https://doi.org/10.1016/j.tins.2018.03.007.

[24] Carter, M.E., Han, S., Palmiter, R.D., 2015. Parabrachial calcitonin gene-related peptide neurons mediate conditioned taste aversion. Journal of Neuroscience 35(11):4582–4586. https://doi.org/10.1523/JNEUROSCI.3729-14.2015.

[25] Liang, N.-C., Bello, N., Moran, T., 2013. Additive feeding inhibitory and aversive effects of naltrexone and exendin-4 combinations. International Journal of Obesity 37(2):272. https://doi.org/10.1038/IJO.2012.16, 2005.

[26] Shah, M., Vella, A., 2014. Effects of GLP-1 on appetite and weight. Reviews in Endocrine & Metabolic Disorders 15(3):181. https://doi.org/10.1007/S11154-014-9289-5.

[27] Walker, C.S., Li, X., Whiting, L., Glyn-Jones, S., Zhang, S., Hickey, A.J., et al., 2010. Mice lacking the neuropeptide α-calcitonin gene-related peptide are protected against diet-induced obesity. Endocrinology 151(9):4257–4269. https://doi.org/10.1210/en.2010-0284.

[28] Liu, T., Kamiyoshi, A., Sakurai, T., Ichikawa-Shindo, Y., Kawate, H., Yang, L., et al., 2017. Endogenous calcitonin gene-related peptide regulates lipid metabolism and energy homeostasis in male mice. Endocrinology 158(5):1194–1206. https://doi.org/10.1210/en.2016-1510.

[29] Soty, M., Vily-Petit, J., Castellanos-Jankiewicz, A., Guzman-Quevedo, O., Raffin, M., Clark, S., et al., 2021. Calcitonin gene-related peptide-induced phosphorylation of STAT3 in arcuate neurons is a link in the metabolic benefits of portal glucose. Neuroendocrinology 111(6):555–567. https://doi.org/10.1159/000509230.

[30] Coester, B., Pence, S.W., Arrigoni, S., Boyle, C.N., Le Foll, C., Lutz, T.A., 2020. RAMP1 and RAMP3 differentially control amylin's effects on food intake, glucose and energy balance in male and female mice. Neuroscience 447. https://doi.org/10.1016/j.neuroscience.2019.11.036.

[31] Marvizón, J.C.G., Pérez, O.A., Song, B., Chen, W., Bunnett, N.W., Grady, E.F., et al., 2007. Calcitonin receptor-like receptor and receptor activity modifying protein 1 in the rat dorsal horn: localization in glutamatergic presynaptic terminals containing opioids and adrenergic α2C receptors. Neuroscience 148(1):250–265. https://doi.org/10.1016/j.neuroscience.2007.05.036.

[32] Palkovits, M., 1983. The rat brain in stereotaxic coordinates. Neuropeptides 3(4):319. https://doi.org/10.1016/0143-4179(83)90049-5.

[33] Garcia, J., Kimeldorf, D.J., Koelling, R.A., 1955. Conditioned aversion to saccharin resulting from exposure to gamma radiation. Science (New York, N.Y.) 122(3160):157–158. https://doi.org/10.1126/science.122.3160.157.

[34] Mietlicki-Baase, E.G., Reiner, D.J., Cone, J.J., Olivos, D.R., McGrath, L.E., Zimmer, D.J., et al., 2015. Amylin modulates the mesolimbic dopamine system to control energy balance. Neuropsychopharmacology 40(2):372–385. https://doi.org/10.1038/npp.2014.180.

[35] Borner, T., Wald, H.S., Ghidewon, M.Y., De Jonghe, B.C., Breen, D., Grill Correspondence, H.J., 2020. GDF15 induces an aversive visceral malaise state that drives anorexia and weight loss. Cell Reports 31(3):107543. https://doi.org/10.1016/j.celrep.2020.107543.

[36] Sclafani, A., Vural, A.S., Ackroff, K., 2017. CAST/EiJ and C57BL/6J mice differ in their oral and postoral attraction to glucose and fructose. Chemical Senses 42(3):259–267. https://doi.org/10.1093/chemse/bjx003.

[37] Konsman, J.-P., 2003. The mouse brain in stereotaxic coordinates. Psychoneuroendocrinology 28(6):827–828. https://doi.org/10.1016/s0306-4530(03)00088-x.

[38] Weir, J.B.d.V., 1949. New methods for calculating metabolic rate with special reference to protein metabolism. The Journal of Physiology 109(1–2):1–9. https://doi.org/10.1113/jphysiol.1949.sp004363.

[39] Even, P.C., Nadkarni, N.A., 2012. Indirect calorimetry in laboratory mice and rats: principles, practical considerations, interpretation and perspectives. American Journal of Physiology - Regulatory, Integrative and Comparative Physiology, 459–476. https://doi.org/10.1152/ajpregu.00137.2012.

[40] Piattini, F., Le Foll, C., Kisielow, J., Rosenwald, E., Nielsen, P., Lutz, T., et al., 2019. A spontaneous leptin receptor point mutation causes obesity and differentially affects leptin signaling in hypothalamic nuclei resulting in metabolic dysfunctions distinct from db/db mice. Molecular Metabolism 25. https://doi.org/10.1016/j.molmet.2019.04.010.

[41] Wielinga, P.Y., Alder, B., Lutz, T.A., 2007. The acute effect of amylin and salmon calcitonin on energy expenditure. Physiology & Behavior 91(2–3):212–217. https://doi.org/10.1016/j.physbeh.2007.02.012.

[42] Spector, A.C., Breslin, P., Grill, H.J., 1988. Taste reactivity as a dependent measure of the rapid formation of conditioned taste aversion: a tool for the neural analysis of taste-visceral associations. Behavioral Neuroscience 102(6):942–952. https://doi.org/10.1037/0735-7044.102.6.942.

[43] Grill, H.J., Norgren, R., 1978. The taste reactivity test. I. Mimetic responses to gustatory stimuli in neurologically normal rats. Brain Research 143(2):263–279. https://doi.org/10.1016/0006-8993(78)90568-1.

[44] Schier, L.A., Hyde, K.M., Spector, A.C., 2019. Conditioned taste aversion versus avoidance: a re-examination of the separate processes hypothesis. PLoS One 14(6):e0217458. https://doi.org/10.1371/journal.pone.0217458.

[45] Pelchat, M.L., Grill, H.J., Rozin, P., Jacobs, J., 1983. Quality of acquired responses to tastes by Rattus norvegicus depends on type of associated discomfort. Journal of Comparative Psychology (Washington, D.C. : 1983 97(2):140–153. https://doi.org/10.1037/0735-7036.97.2.140.

[46] Mitchell, D., Wells, C., Hoch, N., Lind, K., Woods, S.C., Mitchell, L.K., 1976. Poison induced pica in rats. Physiology & Behavior 17(4):691–697. https://doi.org/10.1016/0031-9384(76)90171-2.

[47] Takeda, N., Hasegawa, S., Morita, M., Matsunaga, T., 1993. Pica in rats is analogous to emesis: an animal model in emesis research. Pharmacology, Biochemistry and Behavior 45(4):817–821. https://doi.org/10.1016/0091-3057(93)90126-E.

[48] Borner, T., Workinger, J.L., Tinsley, I.C., Fortin, S.M., Stein, L.M., Chepurny, O.G., et al., 2020. Corrination of a GLP-1 receptor agonist for glycemic control without emesis. Cell Reports 31(11). https://doi.org/10.1016/j.celrep.2020.107768.

[49] De Jonghe, B.C., Horn, C.C., 2009. Chemotherapy agent cisplatin induces 48-h Fos expression in the brain of a vomiting species, the house musk shrew (Suncus murinus). American Journal of Physiology - Regulatory, Integrative and Comparative Physiology 296(4):902–911. https://doi.org/10.1152/ajpregu.90952.2008.

[50] Horn, C.C., Henry, S., Meyers, K., Magnusson, M.S., 2011. Behavioral patterns associated with chemotherapy-induced emesis: a potential signature for nausea in musk shrews. Frontiers in Neuroscience 5(JUL). https://doi.org/10.3389/fnins.2011.00088.

[51] Matsuki, N., Ueno, S., Kaji, T., Ishihara, A., Wang, C.H., Saito, H., 1988. Emesis induced by cancer chemotherapeutic agents in the suncus murinus: a new experimental model. The Japanese Journal of Pharmacology 48(2):303–306. https://doi.org/10.1254/jjp.48.303.

[52] Ueno, S., Matsuki, N., Saito, H., 1987. Suncus murinus: a new experimental model in emesis research. Life Sciences 41(4):513–518. https://doi.org/10.1016/0024-3205(87)90229-3.

[53] Borner, T., Shaulson, E.D., Ghidewon, M.Y., Grill, H.J., Hayes, M.R., De, B.C., et al., 2020. GDF15 induces anorexia through nausea and emesis. Cell Metabolism 31:351–362. https://doi.org/10.1016/j.cmet.2019.12.004.

[54] Borner, T., Shaulson, E.D., Tinsley, I.C., Stein, L.M., Horn, C.C., Hayes, M.R., et al., 2020. A second-generation glucagon-like peptide-1 receptor agonist mitigates vomiting and anorexia while retaining glucoregulatory potency in lean diabetic and emetic mammalian models. Diabetes, Obesity and Metabolism 22(10):1729–1741. https://doi.org/10.1111/dom.14089.

[55] Cheng, W., Gonzalez, I., Pan, W., Tsang, A.H., Adams, J., Ndoka, E., et al., 2020. Calcitonin receptor neurons in the mouse nucleus tractus solitarius control energy balance via the non-aversive suppression of feeding. Cell Metabolism 31(2):301–312. https://doi.org/10.1016/j.cmet.2019.12.012 e5.

[56] Rushing, P.A., Seeley, R.J., Air, E.L., Lutz, T.A., Woods, S.C., 2002. Acute 3rd-ventricular amylin infusion potently reduces food intake but does not produce aversive consequences. Peptides 23(5):985–988. https://doi.org/10.1016/S0196-9781(02)00022-0.

[57] Chance, W.T., Balasubramaniam, A., Chen, X., Fischer, J.E., 1992. Tests of adipsia and conditioned taste aversion following the intrahypothalamic injection of amylin. Peptides 13(5):961–964, 0196-9781(92)90057-A [pii].

[58] Mack, C., Wilson, J., Athanacio, J., Reynolds, J., Laugero, K., Guss, S., et al., 2007. Pharmacological actions of the peptide hormone amylin in the long-term regulation of food intake, food preference, and body weight. American Journal of Physiology - Regulatory, Integrative and Comparative Physiology 293(5): R1855–R1863. https://doi.org/10.1152/ajpregu.00297.2007.

[59] Lutz, T.A., Geary, N., Szabady, M.M., Del Prete, E., Scharrer, E., 1995. Amylin decreases meal size in rats. Physiology & Behavior 58(6):1197–1202. https://doi.org/10.1016/0031-9384(95)02067-5.

[60] Zakariassen, H.L., John, L.M., Lykkesfeldt, J., Raun, K., Glendorf, T., Schaffer, L., et al., 2020. Salmon calcitonin distributes into the arcuate nucleus to a subset of NPY neurons in mice. Neuropharmacology 167. https://doi.org/10.1016/j.neuropharm.2020.107987.

[61] Alhadeff, A.L., Holland, R.A., Zheng, H., Rinaman, L., Grill, H.J., De Jonghe, B.C., 2017. Excitatory hindbrain-forebrain communication is required for cisplatin-induced anorexia and weight loss. Journal of Neuroscience 37(2): 362–370. https://doi.org/10.1523/JNEUROSCI.2714-16.2016.

[62] Liu, M., Zhang, H., Du, B.X., Xu, F.Y., Zou, Z., Sui, B., et al., 2015. Neurokinin-1 receptor antagonists in preventing postoperative nausea and vomiting. Medicine (United States) 94(19). https://doi.org/10.1097/MD.0000000000000762.

[63] Massaro, A.M., Lenz, K.L., 2005. Aprepitant: a novel antiemetic for chemotherapy-induced nausea and vomiting. The Annals of Pharmacotherapy 39(1):77–85. https://doi.org/10.1345/APH.1E242.

[64] Warr, D.G., Hesketh, P.J., Gralla, R.J., Muss, H.B., Herrstedt, J., Eisenberg, P.D., et al., 2005. Efficacy and tolerability of aprepitant for the prevention of chemotherapy-induced nausea and vomiting in patients with breast cancer after moderately emetogenic chemotherapy. Journal of Clinical Oncology 23(12):2822–2830. https://doi.org/10.1200/JCO.2005.09.050.

[65] Dando, T.M., Perry, C.M., 2004. Aprepitant: a review of its use in the prevention of chemotherapy-induced nausea and vomiting. Drugs, 777. https://doi.org/10.2165/00003495-200464070-00013. –94.

[66] Kozáková, Š., Goněc, R., 2010. Aprepitant. Klinicka Farmakologie a Farmacie, 152. https://doi.org/10.2165/11203680-000000000-00000. –4.

[67] Worth, A.A., Shoop, R., Tye, K., Feetham, C.H., D'agostino, G., Dodd, G.T., et al., 2020. The cytokine GDF15 signals through a population of brainstem cholecystokinin neurons to mediate anorectic signalling. Elife 9:1–19. https://doi.org/10.7554/eLife.55164.

[68] Cai, H., Haubensak, W., Anthony, T.E., Anderson, D.J., 2014. Central amygdala PKC-δ+ neurons mediate the influence of multiple anorexigenic signals. Nature Neuroscience 17(9):1240–1248. https://doi.org/10.1038/nn.3767.

[69] Lutz, T.A., Tschudy, S., Rushing, P.A., Scharrer, E., 2000. Amylin receptors mediate the anorectic action of salmon calcitonin (sCT). Peptides 21(2):233–238. https://doi.org/10.1016/S0196-9781(99)00208-9.

[70] Henriksen, K., Byrjalsen, I., Andersen, J.R., Bihlet, A.R., Russo, L.A., Alexandersen, P., et al., 2016. A randomized, double-blind, multicenter, placebo-controlled study to evaluate the efficacy and safety of oral salmon calcitonin in the treatment of osteoporosis in postmenopausal women taking calcium and vitamin D. Bone 91:122–129. https://doi.org/10.1016/j.bone.2016.07.019.

[71] Wisneski, L.A., Croom, W.P., Silva, O.L., Becker, K.L., 1978. Salmon calcitonin in hypercalcemia. Clinical Pharmacology & Therapeutics 24(2):219–222. https://doi.org/10.1002/cpt1978242219.

[72] Enebo, L.B., Berthelsen, K.K., Kankam, M., Lund, M.T., Rubino, D.M., Satylganova, A., et al., 2021. Safety, tolerability, pharmacokinetics, and pharmacodynamics of concomitant administration of multiple doses of cagrilintide with semaglutide 2·4 mg for weight management: a randomised, controlled, phase 1b trial. The Lancet 397(10286):1736–1748. https://doi.org/10.1016/S0140-6736(21)00845-X.

[73] Bettge, K., Kahle, M., Abd El Aziz, M.S., Meier, J.J., Nauck, M.A., 2017. Occurrence of nausea, vomiting and diarrhoea reported as adverse events in clinical trials studying glucagon-like peptide-1 receptor agonists: a systematic analysis of published clinical trials. Diabetes, Obesity and Metabolism 19(3): 336–347. https://doi.org/10.1111/dom.12824.

[74] Sikirica, M.V., Martin, A.A., Wood, R., Leith, A., Piercy, J., Higgins, V., 2017. Reasons for discontinuation of GLP1 receptor agonists: data from a real-world cross-sectional survey of physicians and their patients with type 2 diabetes. Diabetes, Metabolic Syndrome and Obesity: Targets and Therapy 10:403–412. https://doi.org/10.2147/DMSO.S141235.

[75] Smith, K.B., Smith, M.S., 2016. Obesity statistics. Primary Care - clinics in Office practice. p. 121–35. https://doi.org/10.1016/j.pop.2015.10.001.

[76] Rydén, A., Torgerson, J.S., 2006. The Swedish Obese Subjects Study-what has been accomplished to date? Surgery for Obesity and Related Diseases, 549–560 https://doi.org/10.1016/j.soard.2006.07.006.

[77] Wadden, T.A., Butryn, M.L., 2003. Behavioral treatment of obesity. Endocrinology and Metabolism Clinics of North America, 981. https://doi.org/10.1016/S0889-8529(03)00072-0. –1003.

[78] Qiao, Y.C., Ling, W., Pan, Y.H., Chen, Y.L., Zhou, D., Huang, Y.M., et al., 2017. Efficacy and safety of pramlintide injection adjunct to insulin therapy in patients with type 1 diabetes mellitus: a systematic review and meta-analysis. Oncotarget 8(39):66504–66515. https://doi.org/10.18632/oncotarget.16008.

[79] Hoogwerf, B.J., Doshi, K.B., Diab, D., 2008. Pramlintide,the synthetic analogue of amylin: Physiology, pathophysiology, and effects on glycemic control, body weight, and selected biomarkers of vascular risk. Vascular Health and Risk Management, 355–362. https://doi.org/10.2147/vhrm.s1978.

